KU LEUVEN

EEG-based photo diary app: Automatic picture taking in response to state of mind changes

Yi Zhao

Thesis submitted for the degree of Master of Science in Artificial Intelligence, option Engineering and Computer Science

Thesis supervisor:
Prof. dr. ir. Marc Van Hulle

Assessors:
Dr. ir. Benjamin Wittevrongel
Dr. ir. Robin De Croon

Mentor:
Dr. ir. Benjamin Wittevrongel

Academic year 2018 – 2019

Preface

I would like to thank everybody who kept me busy the last year, especially my promoter Prof. Marc Van Hulle and my daily supervisor Benjamin Wittevrongel who provided me with invaluable feedback and help during the whole academic year. I would also like to thank the jury for reading the text. My sincere gratitude also goes to my parents who supported my study in Belgium.

Yi Zhao

Contents

Abstract

The past few decades have witnessed the flourishing development of brain computer interfaces (BCIs). Such systems record and analyse brain responses, and provide meaningful feedback to the user. Typical examples of BCIs are brain-controlled prosthetic limbs, mind-spelling and neuro-steered rehabilitation therapies. In recent years, affective BCIs, which aim to detect emotion from the scalp-recorded signal, have also attracted much attention since these systems not only can assist people with psychiatric disorders, but also combine with other types of BCI components to form hybrid BCI systems to achieve higher robustness.

This study aims to provide theoretical proof-of-concepts for the development of an electroencephalogram (EEG)-based photo diary app. When a heightened emotional state is detected using an EEG-based emotion recognition system, a wireless webcam mounted on the EEG cap or headset would take a time-stamped picture. Such a system can assist patients with disorders of emotional information processing, and could potentially provide valuable insights for caregivers of patients with emotional disorders (e.g., autism).

This study mainly analyzed the relationship between emotion and EEG signals from two perspectives: spectral power of brain rhythms (θ, α and β waves) and multivariate multiscale sample entropy (MMSE). The continuous EEG signal was divided into consecutive partly-overlapping segments, and spectral power of each segment was calculated using the Welch's algorithm. The median power value was used for representing the results of all 32 channels. It is found that the video that elicits amusement showed a significant increment of θ power and the video eliciting sadness showed a significant increment of β power. The elicitation of the emotion "anger" showed a decreased spectral power of all the three rhythms. Before applying the MMSE algorithm, 4 channels (F3, F4, P3, P4) were selected instead of all the 32 channels and a re-sample process was implemented. It is found that the MMSE feature works better in discriminating different emotions (i.e., "amusement", "anger", "sadness" and "tenderness") than in determining whether there is an emotion elicitation or not.

In sum, it is anticipated that spectral power could be used to detect a change of emotions and that the MMSE algorithm could be used for the discrimination of different emotions.

List of Figures and Tables

List of Figures

List of Tables

List of Abbreviations and Symbols

Abbreviations

BCI	Brain-computer interface
EEG	Electroencephalogram
PSD	Power spectral density
MMSE	Multivariate multiscale sample entropy
SVM	Support vector machines

Symbols

Δt1	The first time stage
Δt3	The third time stage
t1	the average θ power in Δt1
t3	the average θ power in Δt3
a1	the average α power in Δt1
a3	average α power in Δt3
b1	the average β power in Δt1
b3	the average β power in Δt3
ϵ	scale factor
$\mathbf{M}$	the embedding vector
$\mathbf{T}$	the time lag vector
r	threshold

Chapter 1

Introduction

In this section, at first, the research background would be briefly introduced. After that, the objectives of the study and corresponding methodology synopsis would be stated. And finally, the structure of the dissertation would be provided.

1.1 Background

The past few decades have witnessed how the brain-computer interface (BCI) technology helped motor- or communication-impaired people "talk" or "walk" again. Brain-computer interface (BCI), also named brain-machine interface (BMI), provides a direct communication pathway between the human brain and the external world [49]. In this way, signals produced due to brain electrical activities containing commands or message could be sent directly to external devices without the participation of peripheral nerves or muscles, which are the normal output pathways of the brain. One of the main applications of BCI technology is to assist patients who are neurologically impaired due to diseases in manipulating neuroprostheses or mentally typing characters as a way of communication. These diseases include but are not limited to, paralysis, amyotrophic lateral sclerosis (ALS), stroke, and brain/spinal cord injuries [29].

The development of BCI is rooted in the exploration of neuroscience. The human nervous system consists of two parts, the central nervous system (CNS) and the peripheral nervous system (PNS) [22]. The CNS consists of the brain and spinal cord whereas the PNS consists primarily of nerves which connect the CNS with the rest of the body. At the cellular level, the nervous system is constructed by two types of cells: neurons (or nerve cells) and glia (or glial cells). Neurons play the role of processing and transmitting signals to other nerve, muscle, or gland cells. Glia, at the same time, protect neurons and also provide structural and metabolic support.

The structure of a typical neuron includes three components: the cell body, dendrites, and axons. The cell body plays no role in neural signaling, but it contains

DNA and directs metabolism. Dendrites receive and integrate synaptic inputs from upstream neurons to the cell body. Axons conduct electrical impulses known as action potentials away from the cell body to the dendrites of downstream cells. It is estimated that the human brain contains around 100 billion neurons [19]. When many neurons in the brain elicit electrical activity synchronously (Figure 1.1), there are electrical potentials generated due to ions (e.g., K+, Na+, Ca+, and Cl-) pumping through neuron membranes [42]. Consequently, brainwaves (or neural oscillations) can be detected both inside and outside the brain scalp.

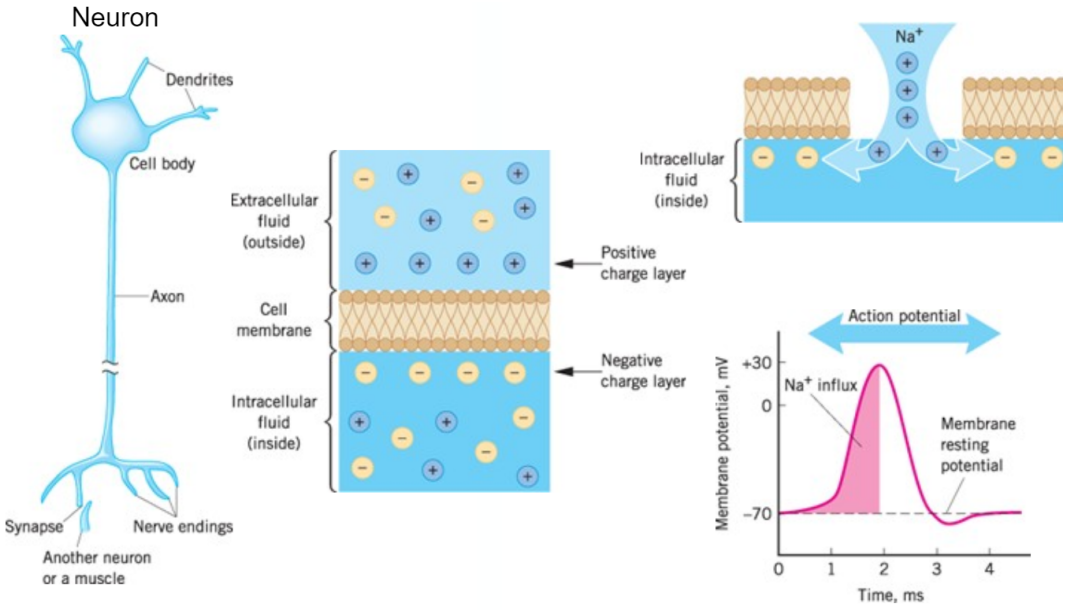

Figure 1.1: Neuron and action potential (Source: Ref. [1])

Generally, BCI can be divided into two main categories based on whether the electrodes are implanted within the brain tissue or not: invasive BCI and non-invasive BCI. The electrode placement is shown in Figure 1.2. The invasive BCI captures signals with a higher signal to noise ratio (SNR). However, the invasive surgical procedure is accompanied with high risks. Non-invasive BCI is therefore preferable for humans in most cases since it is comparably safer, more convenient, and less expensive. Although it captures signals with relatively poor SNR, many experiments have proven that non-invasive BCI is sufficient to provide simple communication pathways for subjects, from controlling a computer cursor [50] to operating a prosthetic device [32].

Leading technologies used in the construction of non-invasive BCIs include electroencephalogram (EEG), magnetoencephalography (MEG), functional magnetic resonance imaging (fMRI), near-infrared spectroscopy (NIRS), and functional transcranial Doppler sonography (fTCD). Nevertheless, EEG is the first and most

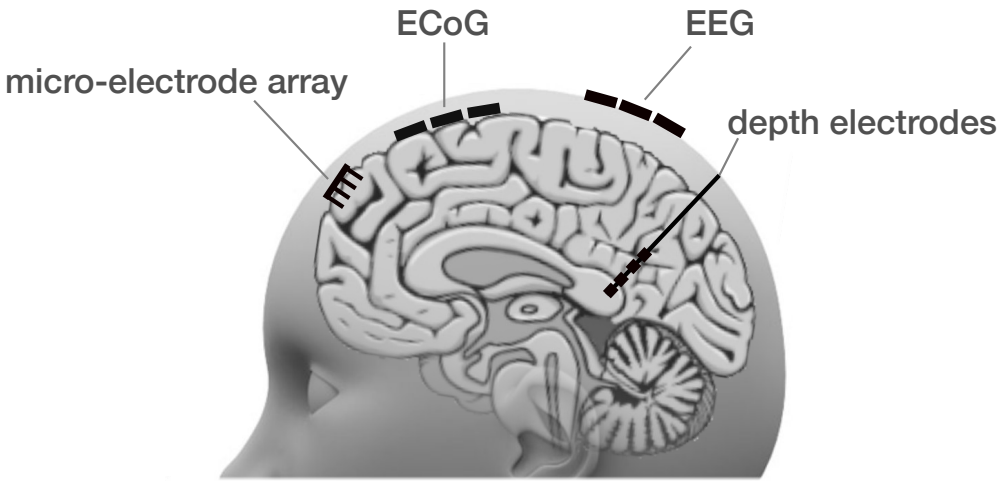

FIGURE 1.2: Different recording electrodes. (Source: Ref. [48])

commonly used one since EEG-based BCI offers higher temporal resolution while it is portable, relatively inexpensive, and easy to use. Consequently, most studies of BCI systems focus on developing EEG-based BCIs.

1.1.1 EEG-based Emotion Analysis

Emotion is a significant integral part of human nature: it influences one's perception of the external world, regulates the behavior of the individual, and even shapes his/her personality. Over the past several decades, many studies on emotion have been conducted from different fields, including neuroscience, psychology, medicine, and so on. Methods for automatic detection and quantitative analysis of emotion make use of information sources such as facial expression, voice, body language, and most importantly, physiological signals (e.g., EEG, ECG).

EEG-based emotion analysis can be applied in developing an affective BCI. Brain, as the central organ of the human nervous system, controls not only body movements or language processing, but also our state-of-mind. Instead of using the voluntary self-regulated brain signals as BCI system inputs to manipulate external devices, it is also suggested that brain signals can be used for analyzing brain states of the subject [35]. The affective BCI can assist people with psychiatric disorders such as Alzheimer's disease and depression. It can also combine with other types of BCI components such as motor imaginary BCI to form hybrid BCI systems which achieve higher robustness [35].

Attempts to recognize emotion using EEG signals have been made from different

perspectives. For example, Aftanas analyzed dimensional complexity and discovered it could discriminate emotion in response to neutral, positive, and negative film clip stimulation [2]. Rosso applied the orthogonal discrete wavelet transform (ODWT) algorithm and defined relative wavelet entropy (RWE) to measure the similarity degree between EEG signal segments. In this way, the dynamics in the EEG stream over time could be presented [39]. Tonoyan combined multivariate empirical mode decomposition (MEMD) and multivariate multiscale sample entropy (MMSE) algorithms to discriminate multiple emotional states (i.e., sadness, amusement, anger, tenderness) [44].

However, for developing a more practical affective BCI system, the methods mentioned above have limitations. Rosso's RWE method is under the precondition that the EEG signal is composed of wavelet components, which is often not the case. Aftanas method is more suitable for off-line analysis and Tonoyan's method requires relatively higher computational resources in the MEMD procedures.

1.2 Objective and Methodology

The goal of this study is to provide theoretical proof of concepts for developing an EEG-based photo diary app. To be more detailed, this app based on a wireless webcam would be mounted on an EEG cap or headset. When an EEG-based BCI component detects emotion changes of the subject, the wireless webcam would take pictures. These pictures can then be time-stamped and collected in a diary. Such an EEG-based emotion diary app could be used for diagnosing and follow-up of patients with dysfunctional processing of emotional information, such as Autism. Moreover, it could also be linked to advanced applications such as emotion-sensitive interactive games, affective interfaces, and emotion-sensitive tutoring systems.

The objectives of this study include two aspects. The first one is to examine the detection of the change of mind (mainly, emotion) over time through a spectrum analysis. A traditional approach in EEG-based emotion analysis is to evaluate the overall power within a given frequency band (i.e., EEG rhythm). However, the reports on which bands matter and how they relate to affective stimuli are still inconclusive. In this study, the spectral power of the theta (θ), alpha(α), and beta (β) rhythms were calculated based on the Welch algorithm. Moreover, the spectral power at different time periods was also compared.

The second objective is to investigate the emotion changes by means of an entropy analysis. It is a more recent approach to relate the intrinsic properties of EEG such as signal complexity to emotional states. This has already been evidenced for a variety of entropy-related metrics, some of which are candidates for real-time implementation. In this study, multivariate multiscale sample entropy (MMSE) was adopted to investigate whether it can distinguish emotions at different time periods.

1.3 Thesis Structure

The remainder of this thesis is structured as follows. Chapter 2 introduces the related literature. Chapter 3 describes the methodology used in this thesis. In Chapter 4, we display the results from experiments as well as give an analysis of those results. In the end, Chapter 5 provides a summary and conclusions.

Chapter 2

Literature Review

There is a large volume of published studies focusing on EEG, emotion, and EEG-based emotion recognition. In this section, main developments in these fields would be described in chronological order.

2.1 EEG

Electroencephalography (EEG) is an electrophysiological modality to record brain electrical signals [34]. It measures voltage fluctuations over a period of time. EEG-based BCI is typically non-invasive with electrodes being placed symmetrically on the scalp, although the invasive version of BCI has also been adopted [23]. Comparing with other non-invasive technologies in measuring brain activity, such as magnetoencephalography (MEG), functional magnetic resonance imaging (fMRI), or near-infrared spectroscopy (NIRS), EEG devices are considered in most BCI systems since it is cheap, portable, and with high temporal resolution [8].

The research on brain waves using EEG signals dates back to 1780s when Galvani first discovered animal electricity [34]. After around one century, Caton observed the electrical phenomena of the exposed cerebral hemispheres of rabbits and monkeys [11]. In 1924, Berger first succeeded in recording EEG signals from the human brain and discovered the alpha wave rhythm. He also invented the term "electroencephalogram". Later on, in 1932, Dietch applied Fourier analysis on EEG recordings. In 1936, Gibbs introduced a new way to diagnose and locate epileptic seizures using EEG, which demonstrated the beginning of clinical electroencephalography [18]. In the same year, Walter detected the "delta wave" and also indicated the possibility of locating active cerebral tumors using this wave. In the 1950s, he also developed EEG topography which provides a foundation for standardizing electrode locations on the scalp [9].

Since 1960, the research of EEG processing algorithms has flourished. In 1970, Hjorth introduced some general characteristics based on the variance for analyzing EEG traces in the time domain. This method is of lower calculation complexity

than the EEG Fourier analysis [20]. In the 1990s, Inouye introduced the concept of entropy, which is a concept in information theory to measure the irregularity of EEG sequences [21]. Schiff applied the wavelet transform, which is a time-frequency analysis method [40]. Pardey described parametric modeling techniques, especially auto-regressive modeling for EEG analysis [28]. Theiler adopted the non-linear chaos theory in an epileptic electroencephalogram and used the Lyapunov exponent for estimation [43]. In 1996, Makeig introduced the independent component analysis (ICA) algorithm to remove noise artifacts. ICA has been widely used among EEG researchers since that time [28].

BCI systems based on EEG properties have also been developed significantly in the past few decades. In the 1980s, Farwell introduced a P300−BCI system which was able to allow "locked-in" patients to communicate at an information rate of 0.2 bps [16]. P300 is an event-related potential (ERP) component. ERP is an electrophysiological response to a meaningful internal or external stimulus first discovered in 1964 [12]. Later on, in 1991, Wolpaw described a BCI system based on the μ rhythm which allowed subjects to move a cursor on screen from the center to left or right [51]. The idea has then been applied in wheelchair control for patients with severe motor deficits. μ rhythm is reported to be blocked by motor imagery [17]. This phenomenon is an example of event-related desynchronization (ERD). After one year, Sutter proposed a VEP-BCI system which required little user training [41]. Visual evoked potential (VEP) was noticed at the early stage of EEG development in the 1930s. A particular case of VEP is steady-state visual evoked potential (SSVEP), which was discovered by Morgan in 1996 [30] and since then SSVEP-BCI systems have been developed considerably.

Despite the fact that EEG signals can be used as system input to manipulate a device (e.g., a cursor on a screen, a wheelchair, or a typing system), they also contain information on mind states (e.g., cognitive states, or emotional states) of subjects [35]. Here are some examples. In the 1960s, Agnew and Williams compared the sleep EEG patterns in late middle age males with that in young adults and found the amount of fourth sleep stage of the elder group showed a noticeable reduction [4] [47]. In the 1980s, Ray found that the alpha wave is strong in tasks not requiring attention while the beta wave is strong in emotional and cognitive tasks [38]. During the same period, by EEG spectral analysis, Ahern discovered the phenomenon hemispherical emotional valence (HEV) which means the left hemisphere is more active for positive emotions while the right hemisphere more for negative emotions [5]. In 1999, Klimesh revealed "alpha desynchronization is positively correlated with (semantic) long-term memory performance, whereas theta synchronization is positively correlated with the ability to encode new information" [25].

2.2 Emotion

Over the past few decades, the amount of studies investigating emotions has increased considerably in different research fields such as medicine, endocrinology, neuroscience, psychology, and cognitive science. One of the earliest theories of emotion named James-Lange theory stated in the 1890s that human emotion is a physiological response to environmental stimulus. After around three decades, another theory of emotion named Cannon-Bard theory argued that physiological reactions and emotion occur simultaneously. According to Kleinginna's work in 1981 [24], emotion can be defined as a complex set of interactions among objective and subjective factors, mediated by neural/hormonal systems, which can adjust mental states and influence individual behaviors. In more detail, it includes:

- giving rise to affective experiences such as feelings of arousal, pleasure/displeasure;
- generating cognitive processes such as emotionally relevant perceptual effects, appraisals, labeling processes;
- activating widespread physiological adjustments to the arousing conditions; and
- leading to behavior that is often, but not always, expressive, goal directed, and adaptive.

For emotion analysis, however, it is challenging to collect physiological data on particular spontaneous emotions. On the one hand, spontaneous emotion cannot be recorded without the procedure of applying sensors, which, might work as a disturbance to subjects and influence collection results. On the other hand, there is no objective ground-truth on emotional states since the self-assessment of subjects is subjective. To tackle this problem, two approaches were proposed for objective evaluation.

The first one is to let subjects assign an emotion category to the induced emotion. Different taxonomies of emotion vary depending on different emotion models. There are two main types of emotion models: the discrete one and the continuous one. Discrete models decompose emotion into several basic core categories. For example, Ekman listed six basic emotion categories: anger, fear, sadness, happiness, disgust, and surprise [15]. Continuous emotion models, however, evaluate emotions on continuous scales. A typical example is the 2−Dimension circumplex valence-arousal model proposed by Russell in 1980 [37]. The horizontal axis represents the pleasure−displeasure dimension while the vertical axis represents the degree−of−arousal dimension. The continuous model, especially this 2−D valence-arousal model, was widely accepted with little controversy. It is easier but it probably more accurate to scale emotion on several dimensions than to decompose it into basic ones.

The second approach is to use pre-validated stimulus databases with high-level of agreement among the population. One of the most popular systems is the International Affective Picture System (IAPS) which is developed by the National Institute

of Mental Health Center for Emotion and Attention at the University of Florida [27]. IAPS provides normative ratings of emotion for around 1000 color photographs. It enables other researchers to customize the stimuli sources for specific experiments.

2.3 EEG-based Emotion Recognition

A considerable amount of literature has been published on algorithms for recognizing emotion in EEG signals. The traditional approach includes two stages: feature extraction and classification. More recently, new methods using deep learning were also proposed, but such techniques require a large amount of input data as well as computational resources [52] [7].

The research of extracting features in EEG signals for recognizing emotion has been flourished over the past two decades. Applying frequency analysis, in 1996, Kostyunina analyzed EEG frequency components when four emotions were induced: sorrow, fear, anger, and joy. It was found that the peak alpha frequency would increase for anger/joy emotions and decrease for sorrow/fear emotions [26]. And in 1997, Musha proposed an emotion matrix making use of the θ, α, and β rhythms to classify four emotional states: relaxation, sadness, anger, and joy [33]. In 2004, Aftanas and co-workers analyzed "the evoked EEG synchronization and desynchronization in the δ, $\theta 1$, $\theta 2$, $\alpha 1$, $\alpha 2$, $\beta 1$, $\beta 2$, $\beta 3$, and γ ranges in response to sequential presentation of stimuli from the International Affective Picture System (IAPS) with low, medium, and high emotional activation impact". They found that both the posterior areas of the right hemisphere and the anterior areas of the left hemisphere were involved in the evoked change of rhythm power. And lower θ range showed smaller time delays than the $\theta 2$, $\alpha 2$, and γ ranges [3]. Based on time-domain signal analysis, in 2000, Vourkas used Hjorth parameters for feature extraction and artificial neural network (ANN) for the classification of three emotions.[46]. More recently, methods based on entropy were proposed. In 2015, Vijayan discussed a new approach to extract features from data using Shannon Entropy and higher order auto-regressive model. Combining with support vector machines (SVM) algorithm, the classification accuracy was 94% [45]. And in 2016, Tonoyan discriminated four emotions (i.e., amusement, anger, tenderness, and sadness) using multivariate multiscale sample entropy (MMSE) based on multivariate empirical mode decomposition (MEMD) successfully [44]. Moreover, in 2018, Mert first applied the MEMD algorithm to decompose the original signal into several intrinsic mode functions (IMFs) and then extracted comprehensive features (related both the time and frequency domain analysis) from the IMFs.

For classification, the traditional methods include Linear Discriminant Function (LDF) and nonlinear SVM. More recently, deep training methods were also used. In 2014, Zheng used models based on a deep belief network (DBN) to classify two emotional categories (positive and negative). This method has achieved classification

accuracy around 87% [52]. In 2017, Alhagry used Long-Short Term Memory (LSTM) to extract features from raw EEG signals and subsequently classify the features into low/high arousal, valence and liking categories [7].

2.4 Conclusion

This chapter reviewed related literature mainly from three parts: EEG, emotion, and EEG-based emotion recognition. The first part mainly includes discoveries of EEG nature and applications in developing EEG-based BCIs. The second part mainly includes definitions and describing methods of emotion. And the third part listed some algorithms proposed for emotion recognition from EEG signals.

Chapter 3

Methodology

In this chapter, research methodologies in EEG-based emotion recognition would be clarified. First of all, the EEG signal analysis follows certain patterns. A general structure for emotion recognition using EEG signals is displayed in Figure 3.1. This chapter is organized based on this structure. There are four sections. Section 1 introduces stimulus sources for emotion induction. Section 2 describes the main points in EEG signal acquisition and preprocessing. Section 3 and Section 4 clarify methods in feature extraction and classification, respectively.

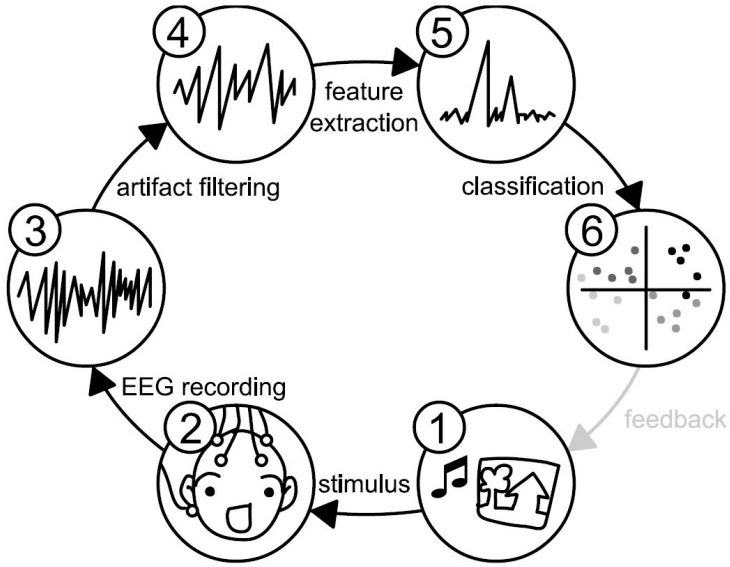

FIGURE 3.1: A General Structure for EEG-based Emotion Recognition (Source: Ref. [10])

3.1 Stimulus

The stimuli used for inducing emotion vary from case to case. As is mentioned in the previous chapter, pre-validated stimulus databases with a high level of agreement among the population are usually selected in emotion-related studies.

The International Affective Picture System (IAPS) containing around 1000 photographs is the most famous example of such databases. The normative emotion ratings were conducted on the Self-Assessment Manikin (SAM, see Figure 3.2), which measures emotion from three dimensions: valence, arousal, and dominance. The first dimension "valence" describes whether the emotion is positive or negative, the second dimension "arousal" describes whether the emotion is active or not, and the third dimension "dominance" describes to which degree the subject feels being controlled.

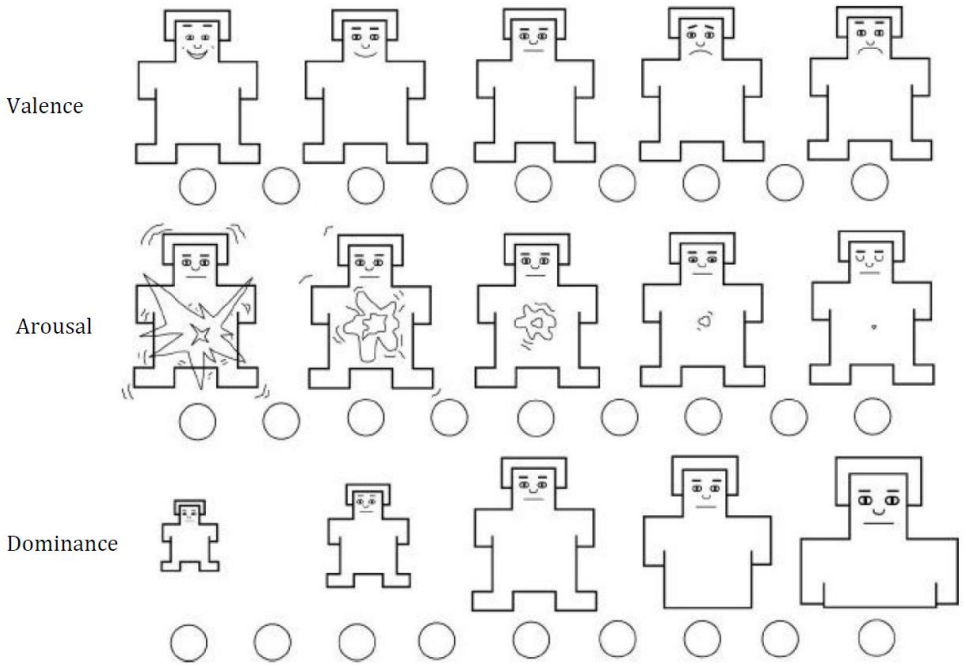

Figure 3.2: Self-assessment Manikin (Source: Ref. [31])

Recently, video stimulus databases have been adopted in more and more studies. On example is the database developed by Schaefer and colleagues (https://sites.uclouvain.be/ipsp/FilmStim/). Each video clip has its "standard label" (i.e., neutral, tenderness, amusement, sadness, fear, anger, or disgust). Around 60 participants self-evaluated the emotional arousal level when watching the videos based on a 7-degree scale. Score "1" meant the participant felt "no emotions at all" and score "7" was corresponding to "very intense emotions".

TABLE 3.1: Video clips used and their standard labels, their mean self-reported emotional arousal levels, standard deviation (SD) and number of participants (N) (Source: [44])

Video clip	Standard label	Mean arousal	SD	N
"Sleepers"	Anger	5.63	1.17	57
"Life is beautiful (4)"	Tenderness	5.59	1.19	50
"City of angels"	Sadness	5.15	1.70	56
"La cité de la peur"	Amusement	4.53	1.75	55

EEG Signal analyzed in this study was recorded when subjects were watching video clips from Schaefer's stimulus database. That is, raw EEG signal recording for analysis was downloaded from https://kuleuven.app.box.com/v/EntropyEmotion. Tonoyan and colleagues created this EEG recording [44]. Tonoyan "selected 4 video clips with top 3 mean self-reported arousal levels from 4 different emotional categories (Table 3.1)". On average, each of the 4 selected video clips lasts for 3 minutes.

3.2 Signal Acquisition

3.2.1 Emotional Brain

The brain is the core of human emotion processing. According to a broadly supported anatomical model, key brain regions for emotion processing include the hypothalamus, prefrontal cortex, anterior cingulate cortex, insular cortex, and amygdala [14]. These brain regions are part of the "limbic system". Figure 3.3 shows a lateral view of its anatomy. The limbic system is not only highly related to emotion, but also other brain functions such as perception, memory, language, autonomic regulation, decision making and so on.

3.2.2 Electrode Placement

To record brain electrical activities using EEG, electrodes are positioned on the scalp. Electrodes are small, disposable, self-adhesive and contain electrode gel. To make sure test outputs for one subject could be effectively analyzed, compiled, and reproduced on others, the international $10-20$ system introduced by Jasper in 1958 was recommended by the International Federation of Societies for Electroencephalography and Clinical Psychophysiology [36]. In this way, specific locations of electrodes could be standardly mapped into specific brain areas (mainly in the cerebral cortex).

As is shown in Figure 3.4, virtual longitude lines terminated by the nasion and the inion are segmented into 6 sections by electrodes, and each section's length is

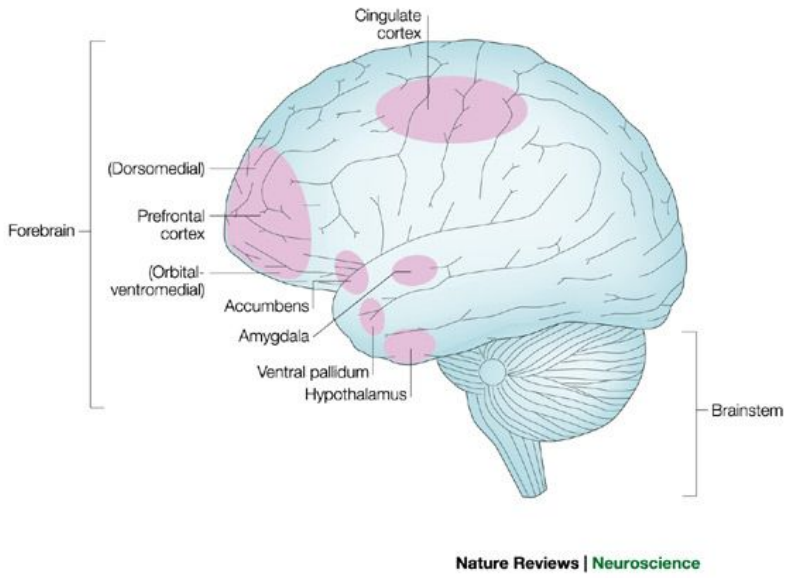

Figure 3.3: Emotional Brain (Source: Ref. [14])

Table 3.2: Electrodes in 10−20 System

Electrode Name	Location
Fp	pre frontal lobe
F	frontal lobe
C	central lobe
T	temporal lobe
P	parietal lobe
O	occipital lobe

10% or 20% of the whole line's. Similarly, the left-right midline terminated by the two ears is also segmented in the same "10−20" manner.

Figure 3.5 is a top view of an extended $10-20$ electrode positioning scheme with 64 scalp sites, which was used in Tonoyan's EEG experiment (i.e., the dataset used in this study). The 32 red positions represent active electrodes where EEG was recorded continuously. The 'z' refers to 'zero' and the corresponding electrodes are placed in the middle. Odd numbers (1, 3, 5, 7, etc.) refer to the corresponding electrodes placed on the left. And even numbers (2, 4, 6, 8, etc.) refer to electrodes on the right. In addition, 'Fp', 'F', 'T', etc. refer to different brain areas, as is described in Table 3.2.

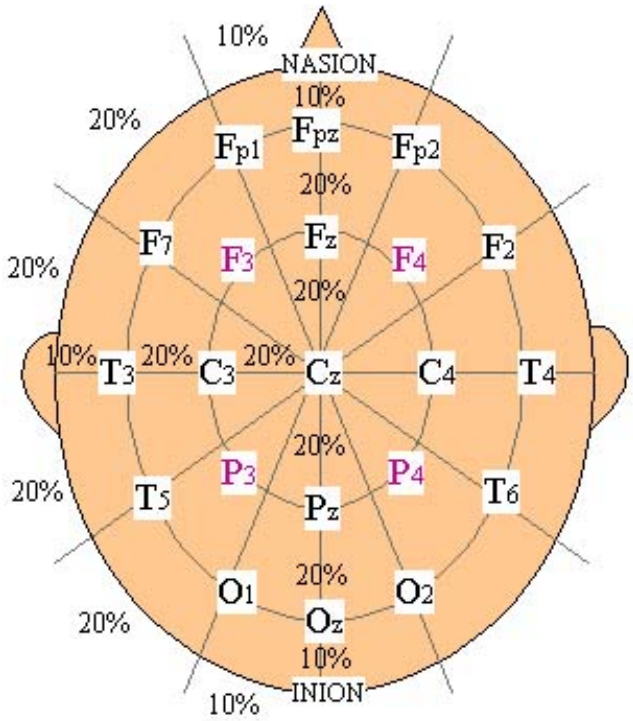

FIGURE 3.4: Electrode Placement in 10−20 System (Source: Ref. [42])

3.2.3 Pre-procession

Noise and artifacts need to be removed for further EEG analysis process. Noise is introduced by sensors or powerline interference during signal recording. Artifacts are generated by other non-task-related physiological activities such as eye movements and blink (i.e., ocular artifact), facial muscle movements (i.e., muscle artifact), etc., which might produce signals even 100 times greater than the EEG signal itself.

In order to collect signals with higher SNR, a pre-amplifier is typically built in the EEG electrodes. In addition, a notching filter is applied to remove the powerline interference noise.

In order to move artifacts, two types of electrodes are used during EEG recording: active electrodes and reference electrodes. The active ones are attached to the scalp in specific locations (e.g. frontal, parietal, occipital, etc.) for detecting neuronal activities while the reference ones mainly work for allowing variations in the potential of an active electrode to be observed [42].

In Tonoyan's EEG experiment, EEG recording was "re-referenced offline from the original common mode sense reference (CMS, positioned next to electrode Pz) to the average of two additional electrodes that were placed on the mastoids of the

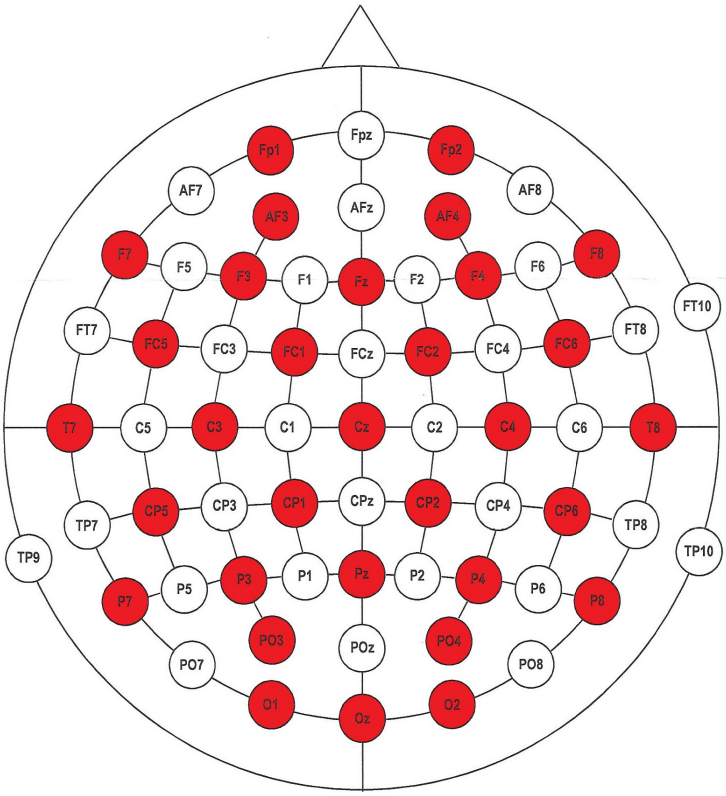

Figure 3.5: 32 electrodes on an extended 10−20 system

subject" [44].

3.3 Feature Extraction

The recorded EEG signal has the following properties:

1. The amplitude is usually smaller than 100 μV (when measured from the scalp and is about 10-20 mV when measured from subdural electrodes).
2. Its frequency mainly ranges from 0.1 to 50 Hz.
3. It is non-stationary and non-linear.
4. It reflects cortical electrical activities.

Generally, the first step to analyze pre-processed EEG data is feature extraction which can be conducted from different perspectives. Hjorth parameters are used in time-domain analysis. Spectrum of EEG rhythms are used in frequency-domain analysis. Wavelet methods try to analyze simultaneously both the time-domain and frequency-domain properties of EEG signals. More advanced algorithms include EMD (empirical mode decomposition), MSE (multiscale sample entropy), etc.. In

TABLE 3.3: Brain Rhythms

Name	Frequency (Hz)	Amplitude (μV)	Brain states
δ	$0.1 \sim 4$	<100	Deep sleep
θ	$4 \sim 8$	<50	Consciousness slips towards drowsiness
α	$8 \sim 12$	<30	Overall mental coordination
β	$12 \sim 30$	<20	Active thinking
γ	$30 \sim 45$	<10	Active cortical processing

this study for developing an EEG-based photo diary, two main branches of EEG feature extraction algorithms were examined: spectral power analysis and entropy analysis.

3.3.1 Spectrum Analysis

Brain Rhythms

Brain waves can be divided into several rhythms defined by frequency: delta (δ) theta (θ), alpha (α), beta (β), and gamma (γ). Past studies have slightly different definitions on the lower and upper bound of each wave band. This study adopts one of the most common definitions, as is listed in Table 3.3.

In addition, an example of the waveforms is displayed in Figure 3.6. Generally, people feel tired, slow, sluggish, or dreamy when slower brainwaves are dominant and wired, or hyper-alert when higher frequencies are dominant.

PSD Estimation using Periodogram

According to the Wiener-Khinchin theorem, for a stationary random signal $x[n]$, its autocorrelation function (ACF) $\varphi_{xx}[n]$ and power spectral density (PSD) $\Phi_{xx}(\omega)$ are Fourier transform pairs:

$$\Phi_{xx}(\omega) \leftrightarrow \varphi_{xx}[n] \tag{3.1}$$

PSD therefore could be calculated based on this relationship. To calculate PSD from N samples of the signal $x\,[n]$, the truncated signal $x_N[n]$ can be denoted as:

$$x_N[n] = x[n] \cdot rect_N[n] \tag{3.2}$$

In this way, the estimated ACF $\hat{\varphi}_{xx}[n]$ is:

$$\hat{\varphi}_{xx}[n] = \frac{1}{N} \cdot x_N[n] * x_N[-n] \tag{3.3}$$

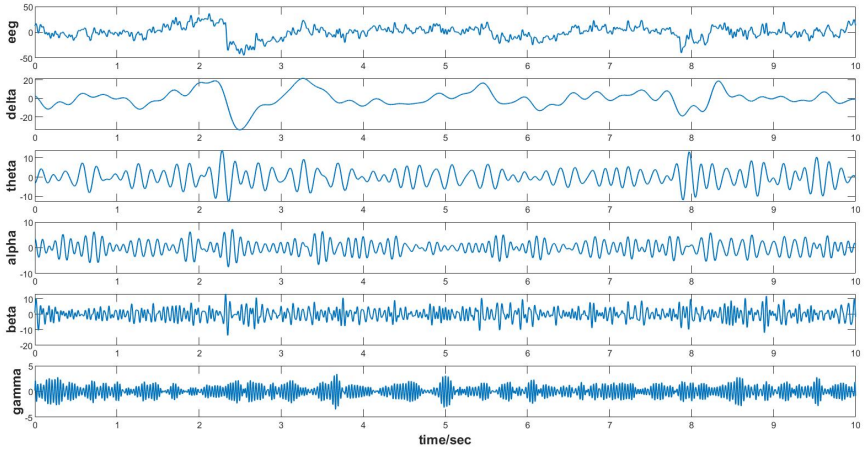

Figure 3.6: Waveforms of EEG Rhythms

Applying DTFT (discrete time Fourier transformation) yields the estimated PSD $\hat{\Phi}_{xx}(\omega)$:

$$\hat{\Phi}_{xx}(\omega) = \frac{1}{N} X_N(\omega) X_N(-\omega) = \frac{1}{N} |X_N(\omega)|^2 \tag{3.4}$$

where $X_N(\omega) = \sum_{n=0}^{N-1} x_N[n] e^{-j\omega n}, n = 0, 1, 2, ..., N-1$.

The Welch's Method

Calculating PSD using Equation 3.4 is the original Periodogram algorithm, which is a non-parametric method. Welch's method is an improved version of the Periodogram algorithm with an estimated result more close to the actual PSD of the signal. It:

1. splits the random signal $x[n]$ into several windowed overlapping segments,
2. estimates the PSD for each segment, and
3. averages over these local estimations.

At first, the random signal $x[n]$ is splited into L overlapping segments $x_l[n]$ of length N, where $l = 0, 1, 2, ..., L-1$. The moving step length is $M \in 1, 2, ..., N$. Each segment is then windowed by the window $w[n]$ with the same length. Therefore, for each windowed $l-$th segment, its DTFT $X_l(\omega)$is:

$$X_l(\omega) = \sum_{n=0}^{N-1} x[n + l \cdot M] w[n] e^{-j\omega n} \tag{3.5}$$

where the window $w[n], n = 0, 1, ..., N-1$ satisfies $\frac{1}{N} \sum_{n=0}^{N-1} |w[n]|^2 = 1$. According to the moving step length M, the overlap is denoted as ratio $\frac{N-M}{N} \cdot 100\%$.
Therefore, the estimated PSD is the average one of all segments:

$$\hat{\Phi}_{xx}(\omega) = \frac{1}{L} \sum_{l=0}^{L-1} \hat{\Phi}_{xx,l}(\omega) \tag{3.6}$$

where $\hat{\Phi}_{xx,l}(\omega)$ represents the estimated PSD of the segment $x_l[n]$ calculated using Periodogram:

$$\hat{\Phi}_{xx,l}(\omega) = \frac{1}{N} |X_l(\omega)|^2 \tag{3.7}$$

It should be noted that the total length of all segments is $(L-1) \cdot M + (N-1)$, which does not exceed the total length of the signal $x[n]$. Otherwise, the last segment $x_{L-1}[n]$ may need to be zero-padded towards length N.

Power of each rhythm

The power of an EEG rhythm is the integral of the PSD over all its range. Therefore:

$$\begin{aligned} P_\theta &= \int_{\omega=\frac{4\cdot 2\pi}{fs}}^{\frac{8\cdot 2\pi}{fs}} \hat{\Phi}(\omega) d\omega \\ P_\alpha &= \int_{\omega=\frac{8\cdot 2\pi}{fs}}^{\frac{12\cdot 2\pi}{fs}} \hat{\Phi}(\omega) d\omega \\ P_\beta &= \int_{\omega=\frac{12\cdot 2\pi}{fs}}^{\frac{30\cdot 2\pi}{fs}} \hat{\Phi}(\omega) d\omega \end{aligned} \tag{3.8}$$

where P_θ, P_α and P_β means the power of the θ, α, and β rhythm, separately. And f_s (in Hz) means the sample rate during signal recording. And $\hat{\Phi}(\omega)$ means the PSD calculated using Welch's method (Equation 3.6).

3.3.2 Entropy Analysis

In Reference [44], Tonoyan used MEMD-based MMSE algorithm and found it can discriminate five emotion states. Channels "F3" and "F4" on the mid-frontal area were selected. In addition, during emotion induction, the complexity level first decreased and then leveled off.

To be more detailed, the MEMD-based MMSE algorithm calculated the MMSE of sequences reconstructed from 15 cumulative intrinsic mode functions (CIMFs). Intrinsic mode function (IMF) is obtained by Empirical Mode Decomposition (EMD). MEMD extended the EMD algorithm and enabled the decomposition of multivariate signals into IMFs. However, MEMD procedure costs a considerable amount of time. Besides, the larger the number of IMFs is, the closer the reconstructed CIMF is to the original signal. Therefore, in this study, the original signal is used for calculating MMSE instead of the reconstructed signal of several main IMFs.

MMSE

Before applying MMSE, the p-variate time sequences need to be pre-processed [6]. It includes:

1. rescaling data to be of values between 0 and 1. That is, for each channel, the j-th data $y(j)$ is replaced by $y_{new}(j)$:

$$y_{new}(j) = \frac{y(j) - min(y)}{max(y) - min(y)} \tag{3.9}$$

   where $j = 1, 2, ..., L$. $min(y)$ is the minimum value of this channel, and $max(y)$ the maximum value of this channel.

2. Z-score. Similarly, the j-th data $y(j)$ is replaced by $y_{new}(j)$:

$$y_{new}(j) = \frac{y(j) - mean(y)}{std(y)} \tag{3.10}$$

   where $j = 1, 2, ..., L$. $mean(y)$ is the mean value of this channel and $std(y)$ the standard deviation.

The procedures for computing MMSE are as follows [6]:
Step 1: Denote the p-variate sequences as $\{y_{k,j}\}_{j=1}^{L}, k = 1, 2, ..., p$. The first step is coarse graining. Let ϵ be the scale factor, the coarse-grained p-variate time sequences $x_{k,i}^{\epsilon}$ are:

$$x_{k,i}^{\epsilon} = \frac{1}{\epsilon} \sum_{j=(i-1)\epsilon+1}^{i\epsilon} y_{k,j} \tag{3.11}$$

where $1 \leq i \leq \frac{L}{\epsilon}$. Besides, let $\frac{L}{\epsilon}$ to be denoted by N. The p-variate time sequences can be denoted as: $\{x_{k,i}\}_{i=1}^{N}, k = 1, 2, ..., p$.

Step 2: The second step is to construct the composite delay vectors based on the $\{x_{k,i}\}_{i=1}^{N}$ sequences. The composite delay vectors $X_m(i)$ are:

$$\begin{aligned} X_m(i) = &[x_{1,i}, x_{1,i+\tau_1}, ..., x_{1,i+(m_1-1)\tau_1}, \\ &x_{2,i}, x_{2,i+\tau_2}, ..., x_{2,i+(m_2-1)\tau_2}, \\ &..., x_{p,i}, x_{p,i+\tau_p}, ..., x_{p,i+(m_p-1)\tau_p}] \end{aligned} \tag{3.12}$$

where $m = \sum_{k=1}^{p} m_k$. $\mathbf{M} = [m_1, m_2, ..., m_p]$ is the embedding vector and $\mathbf{T} = [\tau_1, \tau_2, ..., \tau_p]$ is the time lag vector. Besides, $i = 1, 2, ..., N - n$, where $n = max\{\mathbf{M}\} \times max\{\mathbf{T}\}$.

Step 3: The distances between each pair of the composite delay vectors $X_m(i)$ and $X_m(j)$ are defined by:

$$d[X_m(i), X_m(j)] = \max_{l=1,2,...,m} \{|x(i + l - 1) - x(j + l - 1)|\} \tag{3.13}$$

where $i, j = 1, 2, ..., N$ and $j \neq i$.

Step 4: Given a threshold r, parameters P_i and $B_i^m(r)$ are defined by:

$$P_i = num\left\{d\left[X_m(i), X_m(j)\right] \leq r, j \neq i\right\} \tag{3.14}$$

$$B_i^m(r) = \frac{1}{N-n-1} P_i \tag{3.15}$$

Subsequently, define $B^m(r)$ as:

$$B^m(r) = \frac{1}{N-n} \sum_{i=1}^{N-n} B_i^m(r) \tag{3.16}$$

Step 5: Extend m to be $m+1$, and calculate $B^{m+1}(r)$. Since the sequences are p-variate, there are p different ways. As explained by Ahmed [6], "from a space with the embedding vector $\mathbf{M} = [m_1, m_2, ..., m_p]$, the system can evolve to any space for which the embedding vector is $[m_1, m_2, ..., m_k + 1, ..., m_p](k = 1, 2, ..., p)$. Thus, a total of $p \times (N-n)$ vectors $X_{m+1}(i)$ in $\mathbf{R}^{m+1}$ are obtained, where $X_m(i)$ denotes any embedded vector upon increasing the embedding dimension from m_k to $m_k + 1$ for a specific variable k". In this way, $B_i^{m+1}(r)$ and $B^{m+1}(r)$ are:

$$B_i^{m+1}(r) = \frac{1}{p(N-n)-1} \bullet num\left\{d\left[X_{m+1}(i), X_{m+1}(j)\right] \leq r, j \neq i\right\} \tag{3.17}$$

$$B^{m+1}(r) = \frac{1}{p(N-n)} \sum_{i=1}^{p(N-n)} B_i^{m+1}(r) \tag{3.18}$$

Step 6: At the last step, the MMSE is given:

$$MMSE(\mathbf{M}, \mathbf{T}, r, N) = -ln\left[\frac{B^{m+1}(r)}{B^m(r)}\right] \tag{3.19}$$

3.4 Classification

In this section, at first, a main emotional model adopted in a large number of studies would be introduced. And then, support vector machine (SVM), which is one of the most popular algorithms for classification would also be introduced.

3.4.1 emotion model

As is mentioned in the previous chapter, there are two types of emotion models: the discrete one and the continuous one. The discrete emotion models assign several

basic emotion categories while the continuous models describe emotion from several dimensions.

The circumplex emotion model (shown in Figure 3.7) is widely adopted in many studies. According to Reference [37], it "is consistent with many recent findings from behavioral, cognitive neuroscience, neuroimaging, and developing studies of affects". In this study, the classification would be developed based on this model.

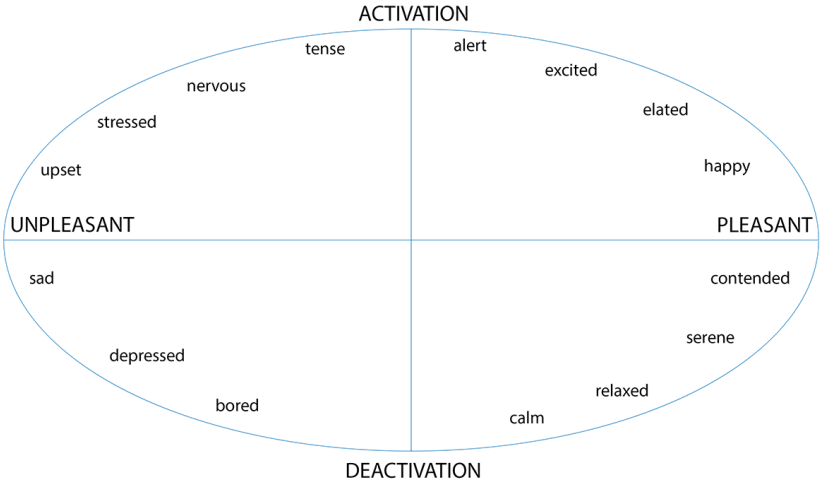

Figure 3.7: Russel's Valence-Arousal Emotion Model (Source: Ref. [37])

3.4.2 SVM

Vapnik proposed the original SVM algorithm in the 1960s. After around thirty years, kernel trick was introduced into this algorithm, which made it more practical [13].

Given a training set $\{x_k, y_k\}_{k=1}^{N}$, where $x_k \in \mathbf{R}^n$ are intput patterns, and $y_k \in \mathbf{R}^n, y_k \in \{-1, +1\}$ are class labels. The classifier can be described as:

$$y\left(x\right) = sign\left[w^T \varphi(x) + b\right] \tag{3.20}$$

with $\varphi(\cdot) : \mathbf{R}^n \to \mathbf{R}^{n_h}$ mapping arguments from original space to high dimensional feature space. w is the weight vector and b the bias. Assume

$$\begin{cases} w^T \varphi\left(x_k\right) + b \geq +1, & if \quad y_k = +1 \\ w^T \varphi\left(x_k\right) + b \leq -1, & if \quad y_k = -1 \end{cases} \tag{3.21}$$

which is equivalent to

$$y_k \left[w^T \varphi\left(x_k\right) + b\right] \geq 1, k = 1, ..., N \tag{3.22}$$

It is an optimization problem (maximize the margin):

$$\min_{w,\xi} J(w,\xi) = \frac{1}{2}w^T w + c\sum_{k=1}^{N}\xi_k \tag{3.23}$$

subject to

$$\begin{cases} y_k\left[w^T\varphi(x_k)+b\right] \geq 1-\xi_k, & k=1,...,N \\ \xi_k \geq 0, & k=1,...,N \end{cases} \tag{3.24}$$

where ξ mean slack variables, which make the classifier more generalized. The primal problem is to estimate w. However, it is usually solved in the dual space by estimating α. The quadratic programming problem (dual problem) is:

$$\min_{\alpha} Q(\alpha) = -\frac{1}{2}\sum_{k,l=1}^{N} y_k y_l K(x_k,x_l)\alpha_k\alpha_l + \sum_{k=1}^{N}\alpha_k \tag{3.25}$$

such that

$$\begin{cases} \sum_{k=1}^{N}\alpha_k y_k = 0 \\ 0 \leq \alpha_k \leq c, \qquad k=1,...,N \end{cases} \tag{3.26}$$

When α is computed, w is calculated using:

$$w = \sum_{k=1}^{N}\alpha_k y_k \varphi(x_k) \tag{3.27}$$

After w being determined, b can be calculated by support vectors.

3.4.3 Other Classification Methods

Although SVM is widely adopted in many studies ([45], [33], ect.), there are types of classification algorithms in machine learning, such as Decision Tree, Naive Bayes, Nearest Neighbor, Neural Network, and so on. The classification toolbox of Matlab offers such classifiers for direct use.

3.5 Conclusion

This chapter described some main methods related to EEG-based emotion recognition, from signal acquisition to signal processing. At first, it introduced the stimuli used in experiments for emotion induction. Second, it described the electrode placement and pre-processing procedures. For feature recognition, it clarified two main methods: the spectrum analysis method (based on Welch's method for calculating PSD) and the entropy analysis method (based on multivariate multiscale sample entropy). Finally, for classification, it introduced the emotional model and explained the SVM algorithm.

Chapter 4

Processes and Results

This section describes the experimental processes and corresponding results during the procedure.

4.1 Raw Dataset

The dataset was downloaded from https://kuleuven.app.box.com/v/EntropyEmotion. It recorded 32-channel EEG signal of 30 subjects when each of them was watching 4 video clips separately. Each video clip is expected to induce a specific emotion (i.e., amusement, anger, sadness, or tenderness). The 32 selected channels were: Fp1, AF3, F7, F3, FC1, FC5, T7, C3, CP1, CP5, P7, P3, Pz, PO3, O1, Oz, O2, PO4, P4, P8, CP6, CP2, C4, T8, FC6, FC2, F4, F8, AF4, Fp2, Fz, and Cz. Their positions across the scalp can be found in Figure 3.5. During the EEG recording, the sample rate was 2048 Hz. Besides, after pre-processing, ocular artifacts were moved.

Figure 4.1 is an example showing the signal of each channel when the emotion amusement was elicited for subject 16. We can also investigate the signal in the frequency domain using fast Fourier transform (FFT), as is shown in Figure 4.2. The simulation result shows the brain waves are low-frequency waves.

4.2 Spectral Power

Since the delta (δ) wave usually appears during deep sleep, and the gamma (γ) wave appears during active cortical processing, this study mainly investigated the theta (θ), alpha (α) and beta (β) rhythms. To be more accurate, we approximately evaluated the change of each rhythm's spectral power over time.

The procedure is as follows:

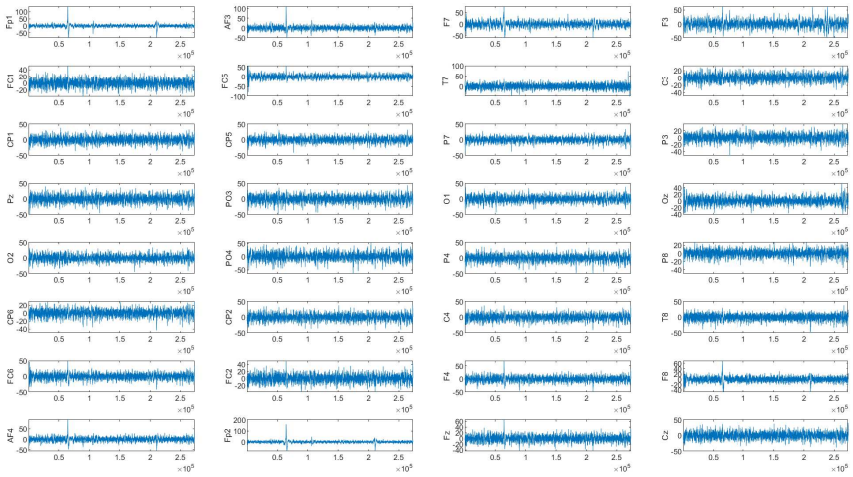

Figure 4.1: Signal after pre-processing (subject: No. 16, emotion: amusement) in time domain. The x−axis represents time (second) and the y−axis represents amplitude (mV).

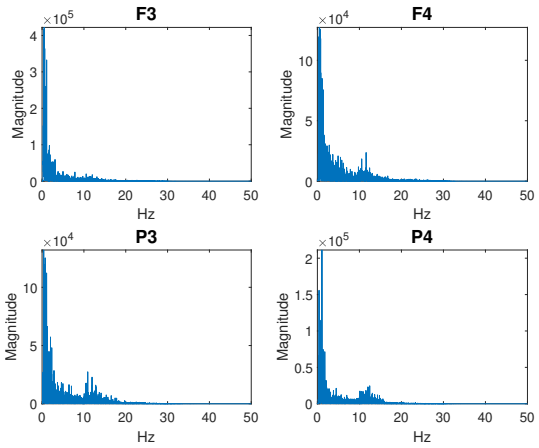

Figure 4.2: Signal of channels "F3", "F4", "P3", "P4" (subject: No. 16, emotion: amusement) in frequency domain after FFT. The x−axis represents frequency (Hz) and the y−axis represents magnitude.

Step 1: Divide the stream signal into time segments. Each segment lasts for $tSeg$ seconds (e.g. 10 sec).

Step 2: Set a move step length $tMov$ (e.g. 1 sec).

Step 3: Calculate the spectral power of theta (θ), alpha (α), and beta (β) rhythms based on Welch's PSD Estimation algorithm for each segment.

Step 4: Examine how spectral power changes over time.

The simulation was conducted with $tSeg = 10sec$ and $tMov = 1sec$. Parameters in the Welch PSD algorithm are: $welchWindowType = "hamming"$, $welchWindowLen = 4096$, $welchWindowMov = 1024$, $welchNoFFT = 4096$. For example, Figure 4.3 depicts the change of theta (θ) power over time when a subject is gradually feeling amused.

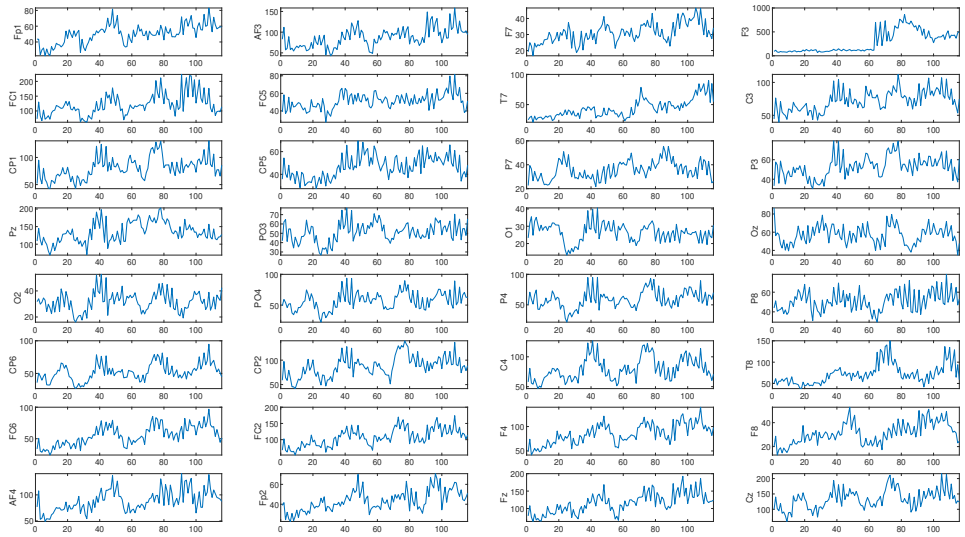

FIGURE 4.3: Spectral Power of theta (θ) rhythm over time (subject: No. 30, emotion: amusement) during the induction of emotion "amusement". The x−axis represents time (second) and the y−axis represents theta power.

From Figure 4.3, it can be seen that the spectral power of EEG signals from different electrodes across the scalp has a similar trend. The neurons synchronization characteristic might explain this phenomenon. Not only the theta (θ) rhythm but also other rhythms (i.e., α, β) showed the power synchronization phenomenon. Some more figures can be found in Appendix A.

If we draw each channel's spectral power in one figure, as is shown in Figure 4.4. The synchronization phenomenon could also be observed while there might exist outliers too. To describe the trends of signals from 32 channels in a simple but accurate way, the median value was used (i.e., the red curve).

4.2.1 Results

Since signals from different subjects have different amplitude, the rhythm spectral power (represented using the median value of all 32 channels) was normalized first. That is, for each sequence, it returns the vector-wise z-score of the data in the

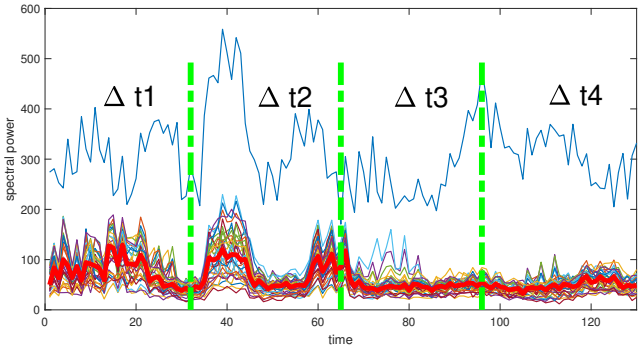

Figure 4.4: Spectral Power of alpha (α) rhythm over time (subject: No. 27, emotion: anger) during the induction of emotion "anger". The red curve is calculated using median value. Four time periods were divided.

sequence with center 0 and standard deviation 1.

Secondly, to measure the change, 4 time periods were determined, as is shown in Figure 4.4. Δt1 represents the beginning period, and Δt3 represents the period when the induced emotion is intense. The dominant of emotion is low at Δt1 and high at Δt3. The average values of spectral power in these two periods are compared. This schedule is shown in Figure 4.5.

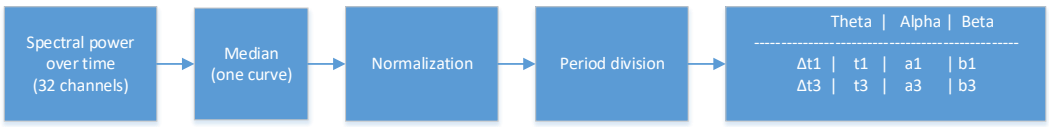

Figure 4.5: Procedures for getting t1 (average θ power in Δt1), t3 (average θ power in Δt3), a1 (average α power in Δt1), a3 (average α power in Δt3), b1 (average β power in Δt1), b3 (average β power in Δt3)

For each subject sample, the 6 parameters (t1, t3, a1, a3, b1, b3) were calculated. t1 is the average θ power at Δt1. t3 is the average θ power at Δt3. a1 is the average α powerat Δt1. a3 is average α power at Δt3. b1 is the average β power at Δt1. And b3 is the average β power at Δt3. The box plot is shown in Figure 4.6.

From Figure 4.6, we may have the following conclusions:

1. Generally, the power of theta (θ), alpha (α) and beta (β) waves increase for emotion "amusement", "sadness" and "tenderness", and decrease for emotion "anger".

2. When people feel amused, the theta (θ) power would have the most significant growth compared with other two rhythms.

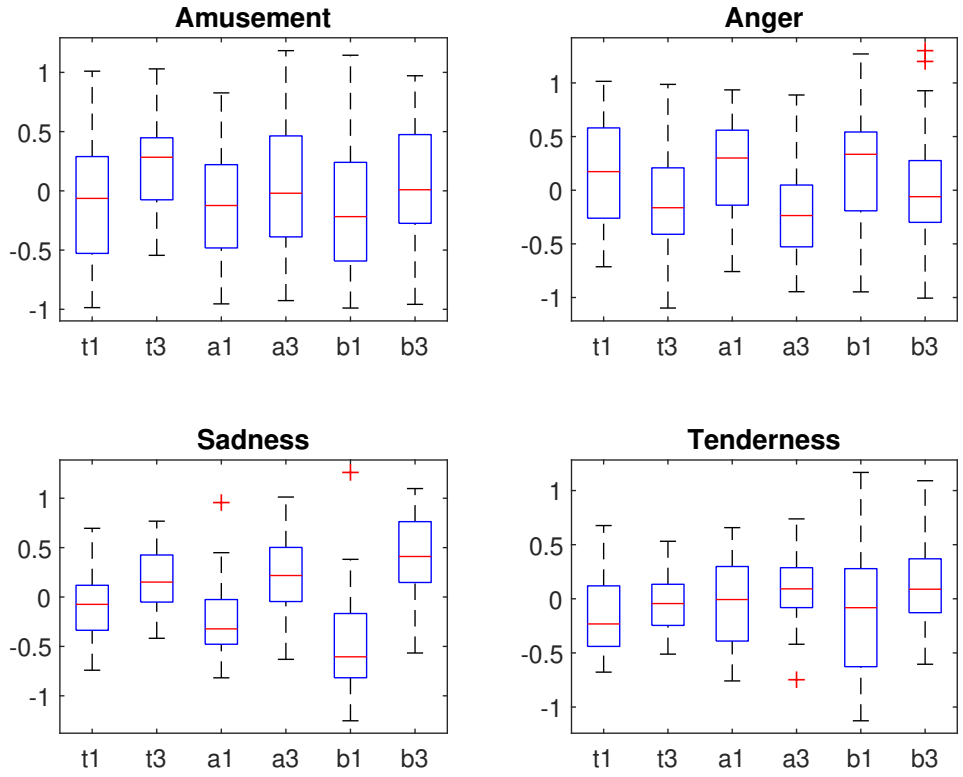

FIGURE 4.6: Box figure of t1, t3, a1, a3, b1, b3 under the four emotions (sample size: 30).

3. For emotion "sadness", beta (β) power would have a distinct increment.

4. For emotion "tenderness", power of all would increase slightly.

4.3 MMSE

Since the MMSE algorithm requires tremendous computational resources especially when the number of channels is large, in this study, 4 channels (F3, F4, P3, P4) were selected instead of all the 32 channels. The selection is due to previous researches that "the anterior areas of the cortex of the left and right hemisphere are associated predominantly with the valence dimension of emotion, while the posterior (especially of the right hemisphere) are associated with the process of emotional activation regardless of valence" [3].

The schedule for computing MMSE is shown in Figure 4.7. For most channels, the original sample rate is 2048Hz. However, it would exceed memory capacities dealing with a significant number of data points. Therefore, in this study, a re-sample process was implemented. And consequently, signals were down-sampled to 256 Hz. Besides, since the frequency of EEG signals is lower than 50Hz, this sample rate

satisfies the Nyquist theory.

After resampling, the data in each channel were rescaled using Equation (3.9) and then normalized using Equation (3.10). During the procedure of coarse graining, let the scale factor ϵ range from 1 to 20. The coarse-grained 4−variate sequences then can be calculated according to the Equation (3.11). Later on, for each ϵ case, multivariate sample entropy was computed. Finally, MMSE values over scale factors ϵ were given.

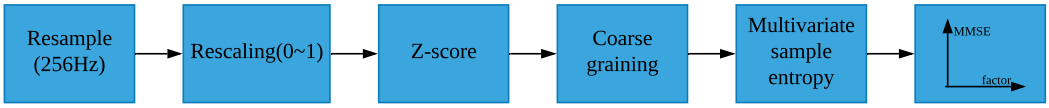

Figure 4.7: Procedures for calculating MMSE over different scale factors (1∼20)

4.3.1 Results

In this study, the embedding vector is $\mathbf{M} = [2, 2, ..., 2]$, the time lag vector is $\mathbf{T} = [1, 1, ..., 1]$, and the threshold is $r = 0.2 \cdot std$ (where std means the standard deviation).

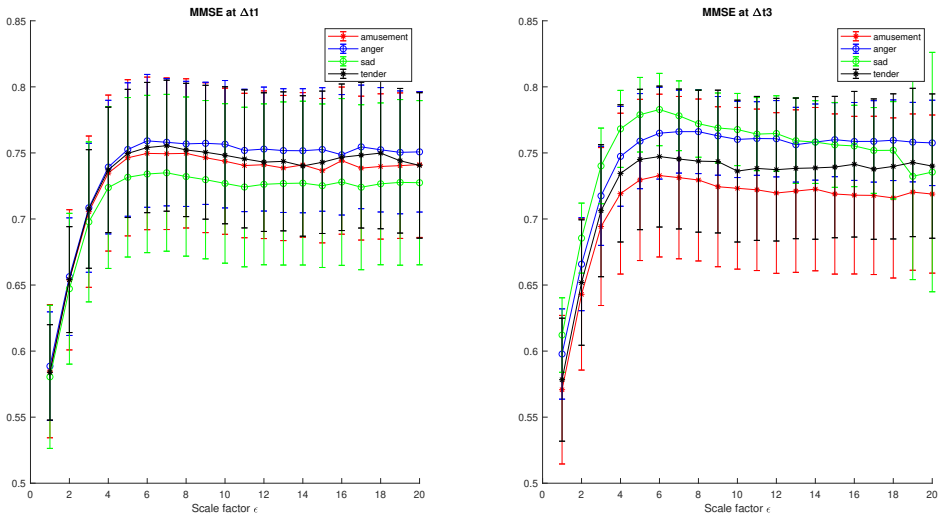

Figure 4.8: MMSE of four emotional states at Δt1 and Δt3

Similar to the procedures in the previous section, four time periods were divided. The MMSE at $\Delta t1$ and $\Delta t3$ were computed. The simulation result is shown in Figure

4.8, from which we may have the following conclusions:

1. Generally, for each emotional state, the change of MMSE at $\Delta t1$ and $\Delta t3$ was tiny.
2. However, it can be seen that at the $\Delta t1$ stage, curves corresponding to the four emotional states were very close while at the $\Delta t3$ stage, they were more separated. It might indicate that MMSE might be able to work as a feature in EEG-based emotion classification.

4.4 Classification

In this study, three classification tasks were implemented. The first one is to classify valence (positive or negative). The second one is to classify arousal (active or nonactive). And the third one is to classify dominant (emotion elicited or not). For the first two tasks, 10-second time segments were selected at the end of Δt3. And for task three, 10-second time segments at Δt1 and Δt3 were both selected. Feature vectors were constructed according to the chosen segments instead of the whole sequences.

The feature vector constructed based on spectral power is:

$$\begin{aligned}[mean(t), max(t), min(t), std(t), mean(a), max(a),\\ min(a), std(a), mean(b), max(b), min(b), std(b)]\end{aligned} \tag{4.1}$$

where t means the median value of theta (θ) power of all channels, a means the median value of alpha (α) power of all channels, and b means the median value of beta (β) power of all channels.

According to Figure 4.8, at time period Δt3, when the scale factor ϵ equals to 5 or 6, the four curves were most separated. Expanding the range a little, the feature vector was constructed based on MMSE is:

$$\begin{aligned}[MMSE(\epsilon = 4), MMSE(\epsilon = 5), MMSE(\epsilon = 6), MMSE(\epsilon = 7),\\ MMSE(\epsilon = 8), MMSE(\epsilon = 9), MMSE(\epsilon = 10)]\end{aligned} \tag{4.2}$$

All these tasks were completed using the classification toolbox of Matlab.

4.4.1 Valence

At first, group the 4 types of emotion into 2 sets: positive and negative. The positive one includes "amusement" and "tenderness" while the negative one includes "anger" and "sadness". Table 4.1 and Table 4.2 show the classification accuracies.

Table 4.1: Classification accuracy for valence when the four emotions were elicited (spectral power features)

Algorithm	Accuracy
Ensemble (Boosted Trees)	56.0%
Quadratic Discrimination	55.2%
SVM (cubic SVM)	54.3%

Table 4.2: Classification accuracy for valence when the four emotions were elicited (MMSE features)

Algorithm	Accuracy
Decision Tree	61.7%
Linear Discrimination	59.2%
SVM (Gaussian SVM)	51.7%

According to Table 4.1 and Table 4.2, the classification accuracies were low for both cases but the MMSE feature outperformed the spectral power feature in discriminating positive/negative emotions.

4.4.2 Arousal

At first, group the 4 types of emotion into 2 sets: high arousal and low arousal. The former includes "amusement" and "anger" while the latter includes "tenderness" and "sadness". Table 4.3 and Table 4.4 show the classification accuracies.

Table 4.3: Classification accuracy for arousal when the four emotions were elicited (spectral power features)

Algorithm	Accuracy
SVM (Quadratic SVM)	53.4%
SVM (cubic SVM)	53.4%

According to Table 4.3 and Table 4.4, similarly, the classification accuracies were low for both cases but the MMSE feature outperformed the spectral power feature in discriminating active/nonactive emotions.

TABLE 4.4: Classification accuracy for arousal when the four emotions were elicited (MMSE features)

Algorithm	Accuracy
SVM (Cubic SVM)	59.2%
SVM (Linear SVM)	58.3%
Linear Discriminant	57.5%

4.4.3 Dominant

This dominant classification task aims at classifying the input feature vector into two classes: emotion elicited and emotion not elicited. Input data which is corresponding to the Δt1 stage was label "+1" and which is corresponding to the Δt3 stage was label "-1". Table 4.5 and Table 4.6 show the classification accuracies.

TABLE 4.5: Classification accuracy for dominant: whether emotion is induced or not (spectral power features)

Algorithm	Accuracy
Naive Bayes	54.7%
Logistic Regression	54.7%
SVM (Gaussian SVM)	51.3%

TABLE 4.6: Classification accuracy for dominant: whether emotion is induced or not (MMSE features)

Algorithm	Accuracy
Naive Bayes	55.0%
Decision Tree	52.1%

According to Table 4.3 and Table 4.4, the classification accuracies were low for both cases and the two features performed similarly.

4.5 Conclusion

This chapter described the experimental processes and simulation results. This first section described the data. The second section showed the implementation of spectral power analysis. The third section showed the implementation of entropy

analysis. And the fourth section listed the classification accuracies using spectral power features and entropy features.

Chapter 5

Conclusion

The goal of this study is to provide theoretical proof of concepts for developing an EEG-based emotion diary app. Two sub-goals were developed based on this goal. One is to detect the changes of emotion over time. If the changes of emotion can be detected then the photos in the app can be time-stamped. The other goal is to determine the type of the induced emotion. It would make the diary app more informative and useful.

The analysis was conducted from two aspects: spectral power and entropy. For the spectral power aspect, this study investigated the power of θ, α, and β rhythms which were calculated according to Welch's method. For the entropy aspect, this study investigated the MMSE of the signals.

5.1 Findings

From the spectral power analysis, it is found that when the emotion "anger" was induced, theta (θ), alpha(α) and beta (β) power would decrease, while for the other three types of emotion ("amusement", "sadness", and "tenderness"), power of these rhythms would increase. Besides, when the emotion "amusement" was induced, the θ power had the most significant increment. Similarly, when the emotion "sadness" was induced, the β power had the most significant increment. For the emotion "tenderness", power of all rhythms increased slightly compared with the beginning stage (when subjects were peaceful and had no strong emotions).

From the entropy analysis, it is found that for each emotion, the MMSE values at the beginning stage and at the stage when emotion was strong didn't have an obvious difference. However, it can clearly be seen that at the beginning stage, the MMSE values of the four emotional states were very close, while later in the videos (i.e., when the emotional context was more pronounced), the four MMSE values were more separated. This indicates that MMSE might be able to work as a feature for

discriminating different types of emotion.

Using spectral power and MMSE as features for emotion recognition, in this study, both features showed low classification accuracies. However, it is also found that MMSE outperforms spectral power in classifying emotion types (i.e. positive or negative, active or nonactive). But in detecting whether there is an emotional change (i.e. emotion induced or emotion not induced), these two features have similar classification accuracies.

5.2 Discussion

This work contributes to existing knowledge that the change of emotion is related to the change of frequency powers and complexity of scalp-recorded brain signals. These findings offer suggestions for the development of an on-line EEG-based affective BCI system. For example, a significant increment of β power might indicate that the person wearing this EEG-based affective BCI system feels sad (comparing with the baseline).

A limitation of this study is that the simulation results in classifying different emotions were not very satisfying. Further work could be conducted after collecting more data. Or more questions can be explored such as what arguments to use in constructing feature vectors based on spectral power or entropy, and so on.

Appendices

Appendix A

Each Channel's Spectral Power Over Time Under Four Emotions

Here are some figures showing spectral power of signals from the whole 32 channels over time. There are 12 combinations of Rhythm (i.e. θ, α, β) and emotion (i.e. amusement, anger, sadness, tenderness). For each combination, one subject's EEG recording is presented.

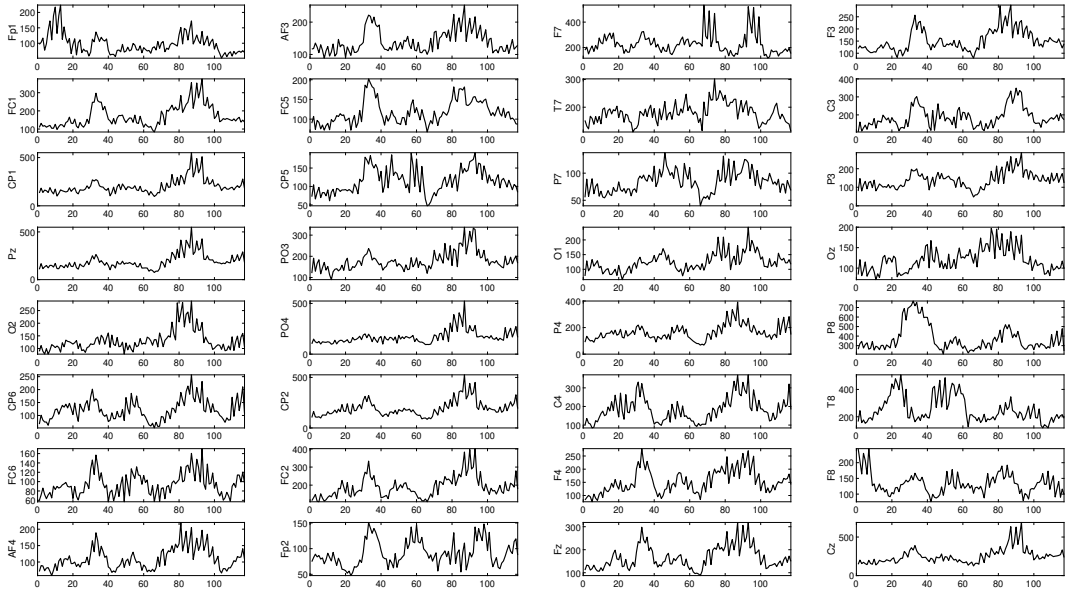

FIGURE A.1: Spectral Power of theta (θ) rhythm over time (subject: No. 5, emotion: amusement) during the induction of emotion "amusement".

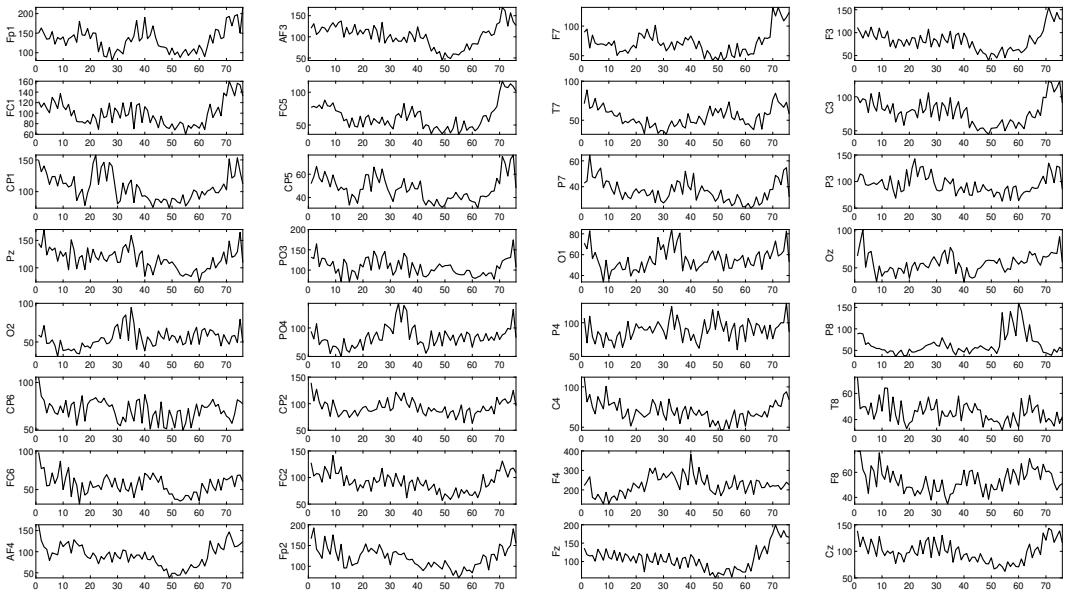

Figure A.2: Spectral Power of theta (θ) rhythm over time (subject: No. 7, emotion: anger) during the induction of emotion "anger".

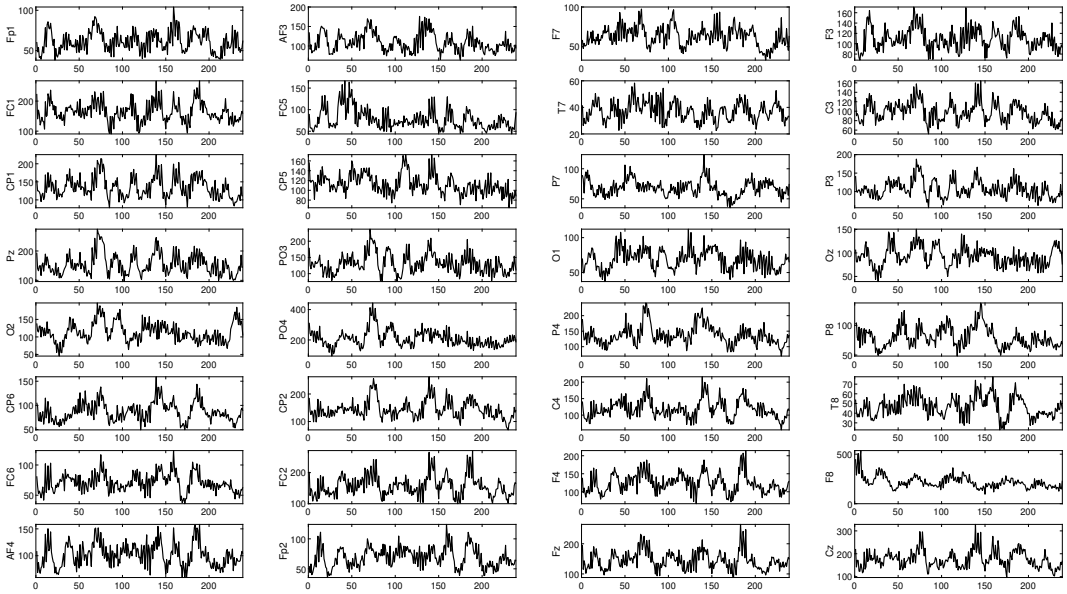

Figure A.3: Spectral Power of theta (θ) rhythm over time (subject: No. 13, emotion: sadness) during the induction of emotion "sadness".

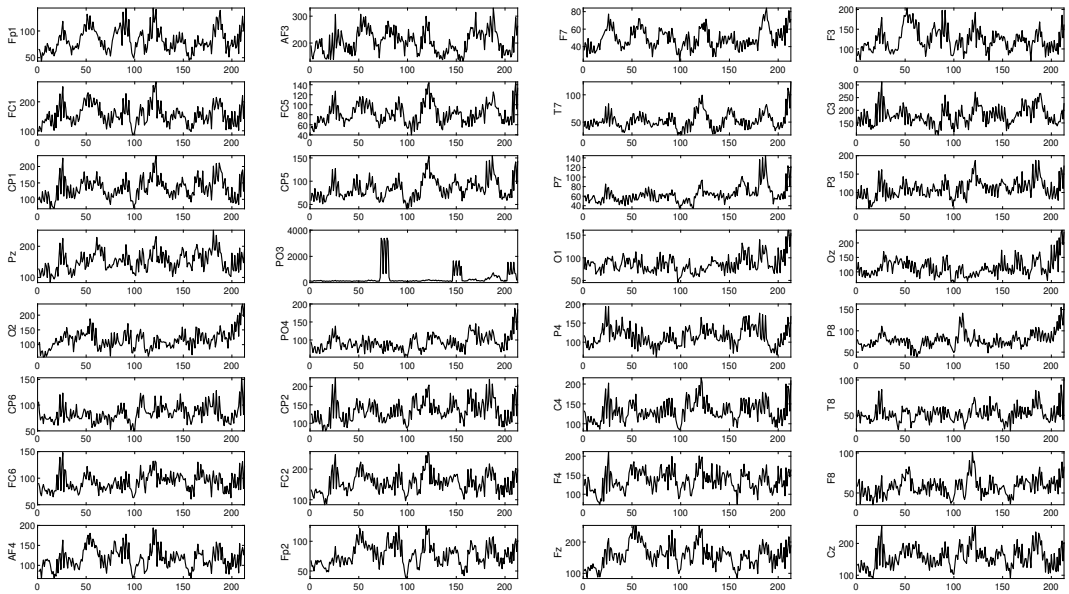

FIGURE A.4: Spectral Power of theta (θ) rhythm over time (subject: No. 24, emotion: tenderness) during the induction of emotion "tenderness". For this case, the channel "PO3" need to be removed.

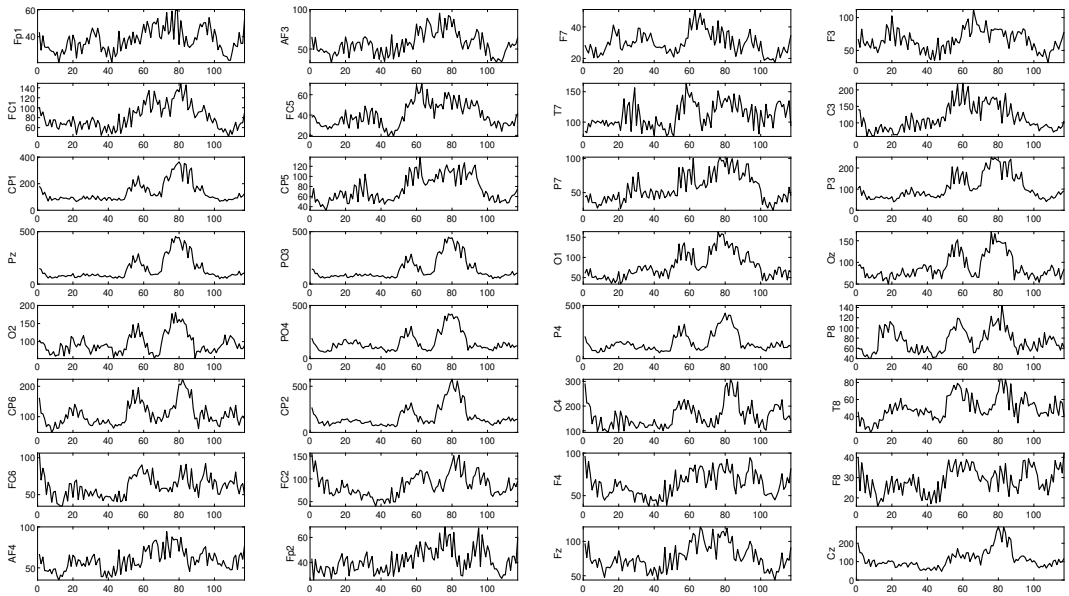

FIGURE A.5: Spectral Power of alpha (α) rhythm over time (subject: No. 1, emotion: amusement) during the induction of emotion "amusement".

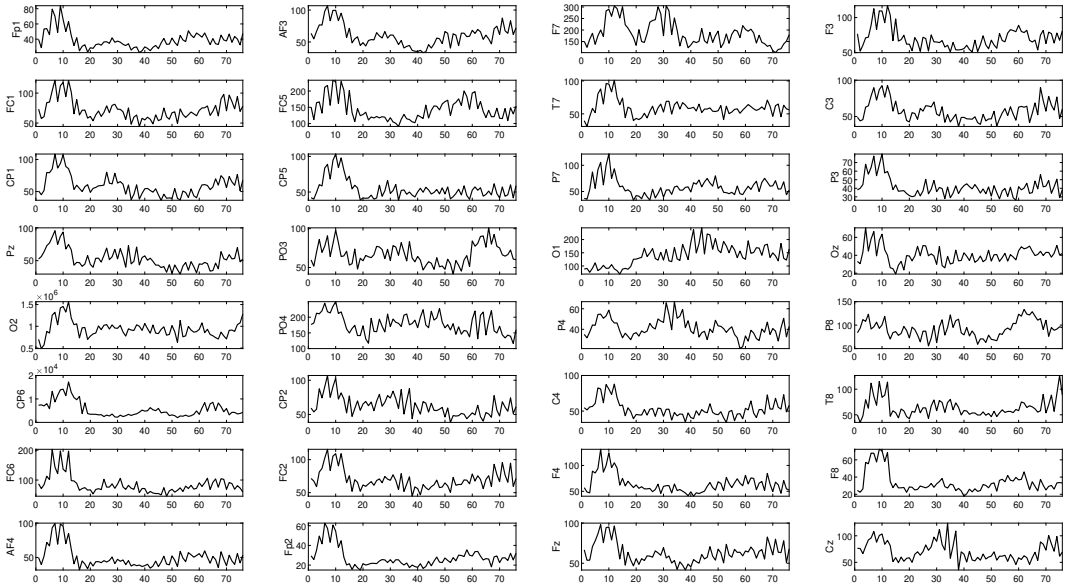

Figure A.6: Spectral Power of alpha (α) rhythm over time (subject: No. 6, emotion: anger) during the induction of emotion "anger".

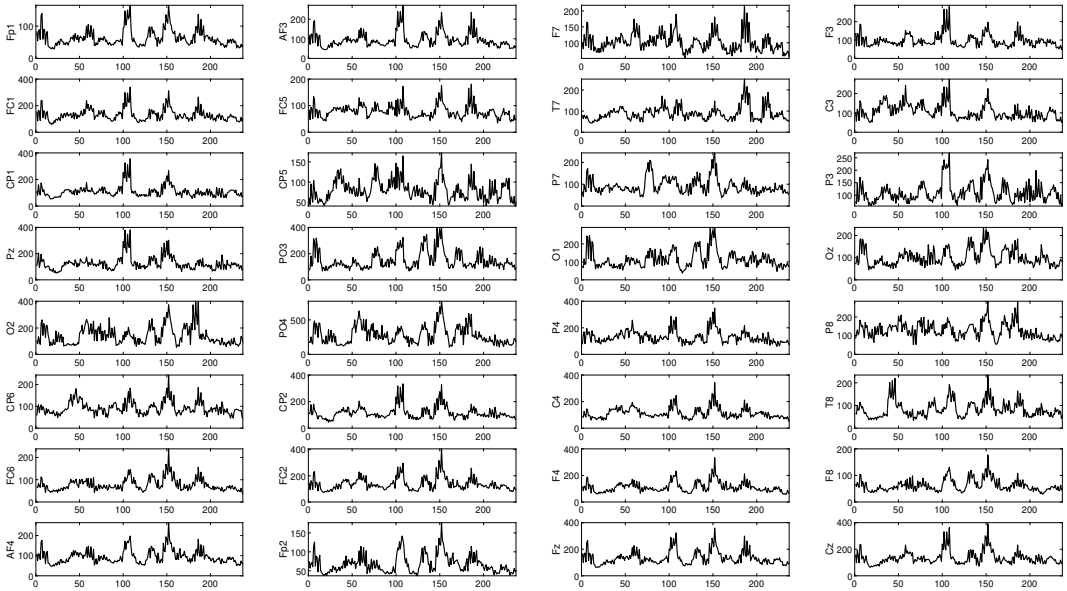

Figure A.7: Spectral Power of alpha (α) rhythm over time (subject: No. 16, emotion: sadness) during the induction of emotion "sadness".

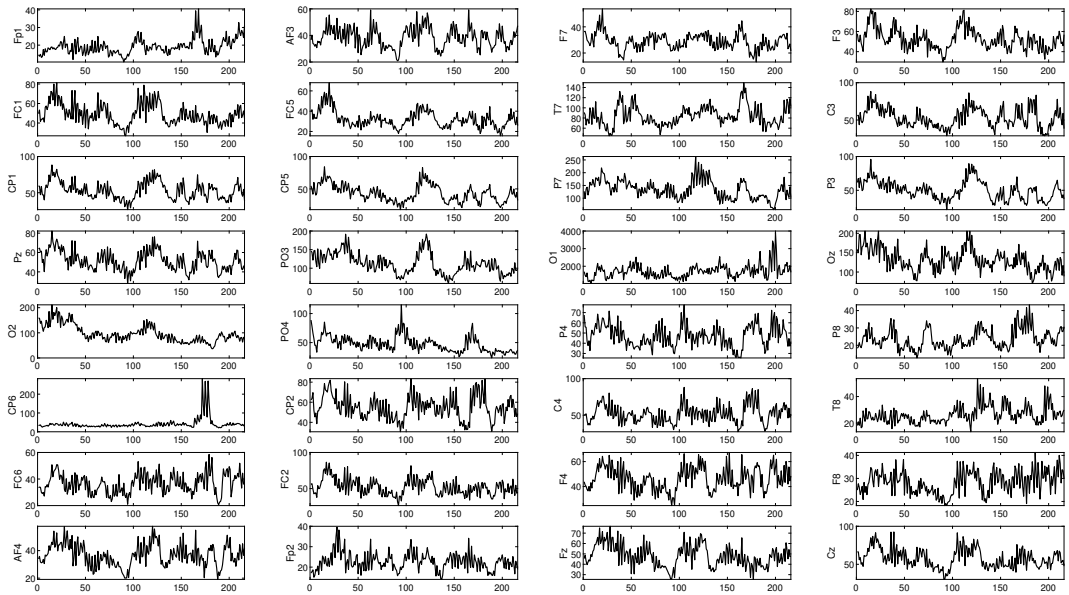

FIGURE A.8: Spectral Power of alpha (α) rhythm over time (subject: No. 20, emotion: tenderness) during the induction of emotion "tenderness". For this case, the channel "CP6" need to be removed.

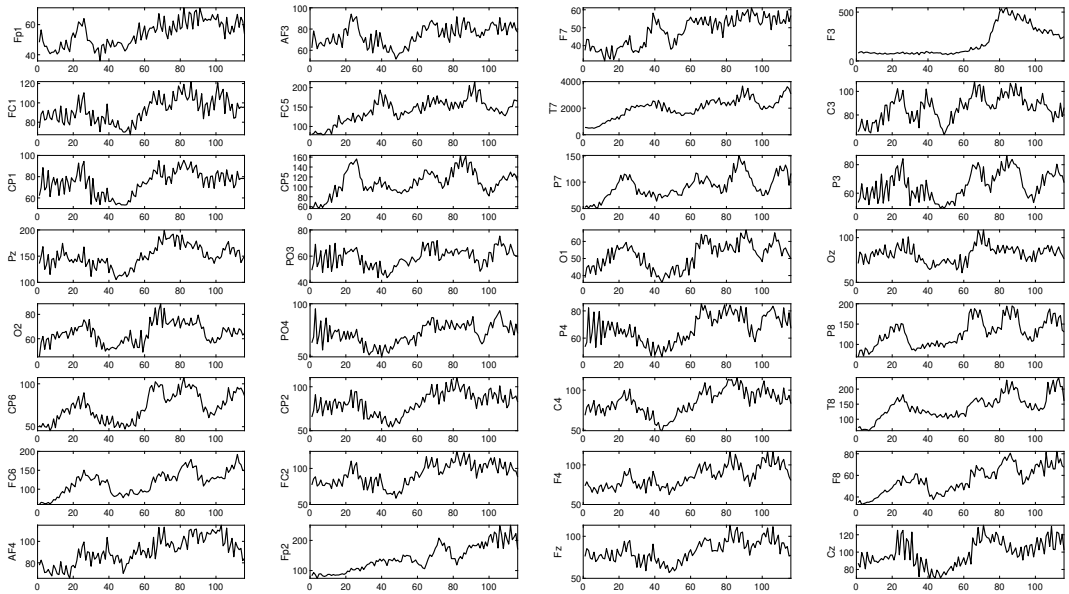

FIGURE A.9: Spectral Power of beta (β) rhythm over time (subject: No.30, emotion: amusement) during the induction of emotion "amusement".

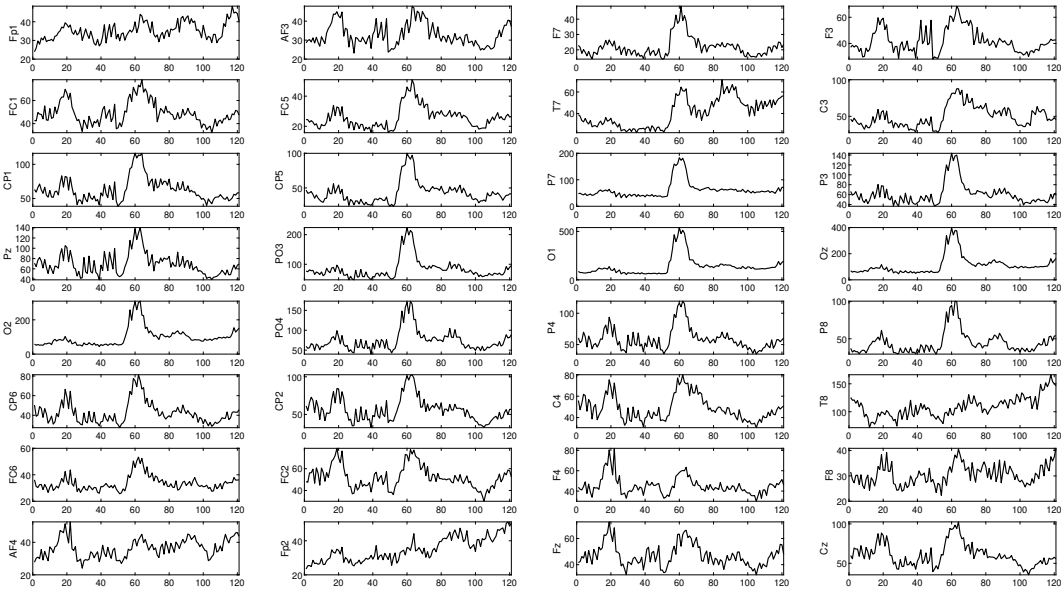

Figure A.10: Spectral Power of beta (β) rhythm over time (subject: No. 25, emotion: anger) during the induction of emotion "anger".

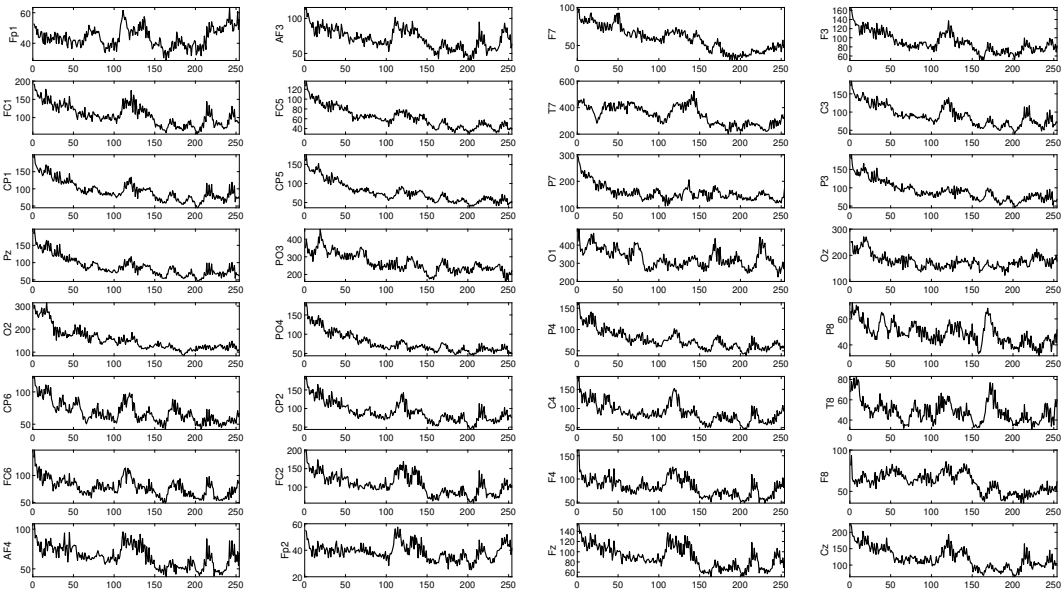

Figure A.11: Spectral Power of beta(β) rhythm over time (subject: No. 20, emotion: sadness) during the induction of emotion "sadness".

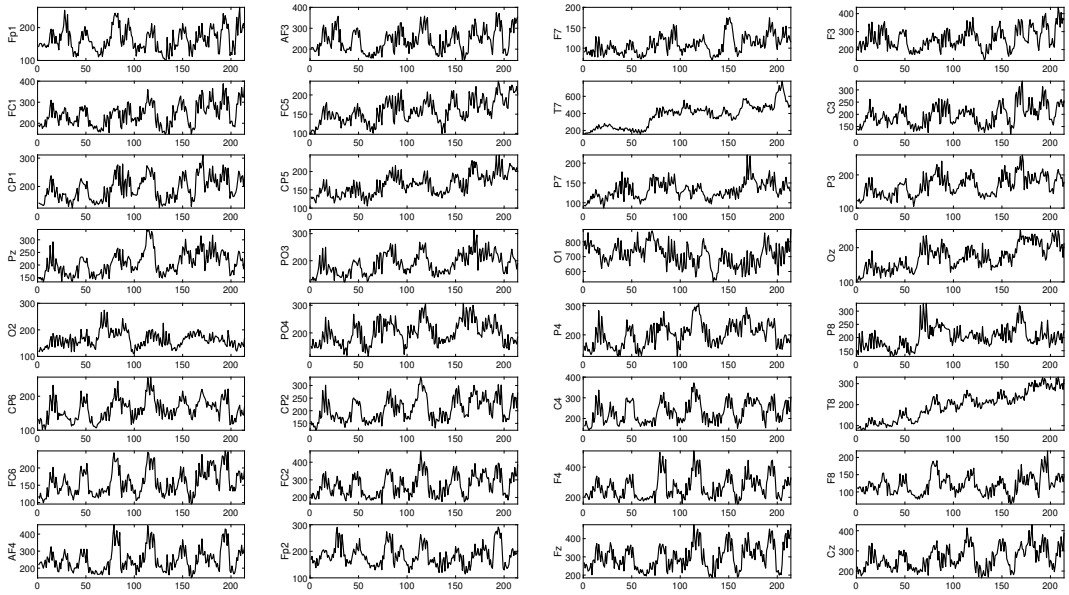

FIGURE A.12: Spectral Power of beta (β) rhythm over time (subject: No. 27, emotion: tenderness) during the induction of emotion "tenderness".

Appendix B

The Codes for Main functions

B.1 Spectral Power based on Welch Algorithm

The function `TABWelch` calculates the spectral power of the θ, α, β rhythms using the Welch Periodogram algorithm.

```
function [Theta, Alpha, Beta]=TABWelch(fileName)
load(fileName);
Beta=[];
Alpha=[];
Theta=[];
for j=1:32
scs=processedEEG(j,:); %scs: single channel signal
pt=1;%pt: point
theta_power=[];
alpha_power=[];
beta_power=[];
while(pt+sampleRate*10<length(scs))
x=scs(pt:pt+sampleRate*10); % Segment length: 10 secondes
[pxx,f]=pwelch(x,hamming(2*sampleRate),0.5*sampleRate,length(x),sampleRate);
%[pxx,f] = pwelch(x,window,noverlap,nfft,fs)
theta_power=[theta_power sum(pxx(find(f>=4 & f<=8)))];
alpha_power=[alpha_power sum(pxx(find(f>=8 & f<=12)))];
beta_power=[beta_power sum(pxx(find(f>=12 & f<=30)))];
pt=pt+sampleRate*1; % Move step length: 1 second
end
Beta=[Beta; beta_power];
Alpha=[Alpha;alpha_power];
Theta=[Theta;theta_power];
end
```

B.2 MMSE

The function `MMSE4channels` calculates the MMSE of four-channel sequences. The scale factor ϵ ranges from 1 to 20.

```
function result=MMSE4channels(x)
result=[];
[n,b]=size(x);
for ch=1:4
m=min(x(:,ch));
M=max(x(:,ch));
x(:,ch)=(x(:,ch)-m)/(M-m);
end

x=zscore(x);
sd = sum(std(x));
r = 0.2*sd;
epsilon=20;
for j=1:epsilon
for p=1:b
for i=1:n/j
y(i)=0;
for k=1:j
y(i)=y(i)+x((i-1)*j+k,p);
end
y(i)=y(i)/j;
end
z=y(1:floor(n/j));
X(:,p)=z;
end
M = 2*ones(1,4);
tau=ones(1,4);
e=mvsampen_full(M,r,tau,X');
SE(j)=e;
clear X;
end
result=[result;SE]
```

The function `mvsampen_full(M,r,tau,ts)` (Reference [6]) works for calculating the multivariate sample entropy.

```
function e=mvsampen_full(M,r,tau,ts)
% Inputs:

% M - embedding vector parameter
% r - threshold scalar parameter
```

```
% tau - time lag vector parameter
% ts - multivariate time series-a matrix of size nvarxnsamp

% Output:
% e- scalar quantity

mm=max(M);
mtau=max(tau);
nn=mm*mtau;


[nvar,nsamp]=size(ts);
N=nsamp-nn;
A=embd(M,tau,ts);
y=pdist(A,'chebychev');
[r1,c1,v1]= find(y<=r);
p1=numel(v1)*2/(N*(N-1));
clear  y r1 c1 v1 A;

M=repmat(M,nvar,1);
I=eye(nvar);
M=M+I;

B=[];

% number of match templates of length m+1
%closed within the tolerance r where m=sum(M) is calculated afterwards
for h=1:nvar
Btemp=embd(M(h,:),tau,ts);
B=vertcat(B,Btemp);
Btemp=[];
end
z=pdist(B,'chebychev');
[r2,c2,v2]= find(z<=r);
p2=numel(v2)*2/(nvar*N*(nvar*N-1));
clear  z r2 c2 v2 B;
e=log(p1/p2);
```

Bibliography

[1] Potential energy and electric potential. https://slideplayer.com/slide/8757185/, 2010. Accessed: 05-June-2019.

[2] L. I. Aftanas, N. V. Lotova, V. I. Koshkarov, V. P. Makhnev, Y. N. Mordvintsev, and S. A. Popov. Non-linear dynamic complexity of the human eeg during evoked emotions. *International Journal of Psychophysiology*, 28(1):63–76, 1998.

[3] L. I. Aftanas, N. V. Reva, A. A. Varlamov, S. V. Pavlov, and V. P. Makhnev. Analysis of evoked eeg synchronization and desynchronization in conditions of emotional activation in humans: temporal and topographic characteristics. *Neuroscience and behavioral physiology*, 34(8):859–867, 2004.

[4] H. W. Agnew Jr, W. W. Webb, and R. L. Williams. Sleep patterns in late middle age males: an eeg study. *Electroencephalography and clinical neurophysiology*, 23(2):168–171, 1967.

[5] G. L. Ahern and G. E. Schwartz. Differential lateralization for positive and negative emotion in the human brain: Eeg spectral analysis. *Neuropsychologia*, 23(6):745–755, 1985.

[6] M. U. Ahmed and D. P. Mandic. Multivariate multiscale entropy analysis. *IEEE signal processing letters*, 19(2):91–94, 2011.

[7] S. Alhagry, A. A. Fahmy, and R. A. El-Khoribi. Emotion recognition based on eeg using lstm recurrent neural network. *Emotion*, 8(10):355–358, 2017.

[8] S. Amiri, R. Fazel-Rezai, and V. Asadpour. A review of hybrid brain-computer interface systems. *Advances in Human-Computer Interaction*, 2013:1, 2013.

[9] P. F. Bladin. W. grey walter, pioneer in the electroencephalogram, robotics, cybernetics, artificial intelligence. *Journal of clinical neuroscience*, 13(2):170–177, 2006.

[10] D. O. Bos et al. Eeg-based emotion recognition. *The Influence of Visual and Auditory Stimuli*, 56(3):1–17, 2006.

[11] R. Caton. Electrical currents of the brain. *The Journal of Nervous and Mental Disease*, 2(4):610, 1875.

[12] R. M. Chapman and H. R. Bragdon. Evoked responses to numerical and non-numerical visual stimuli while problem solving. *Nature*, 203(4950):1155, 1964.

[13] C. Cortes and V. Vapnik. Support-vector networks. *Machine learning*, 20(3):273–297, 1995.

[14] T. Dalgleish. The emotional brain. *Nature Reviews Neuroscience*, 5(7):583, 2004.

[15] P. Ekman. An argument for basic emotions. *Cognition & emotion*, 6(3-4):169–200, 1992.

[16] L. A. Farwell and E. Donchin. Talking off the top of your head: toward a mental prosthesis utilizing event-related brain potentials. *Electroencephalography and clinical Neurophysiology*, 70(6):510–523, 1988.

[17] H. Gastaut, R. Naquet, and Y. Gastaut. A study of mu rhythm in subjects lacking one or more limbs. *Electroencephalography and Clinical Neurophysiology*, 18(7):720, 1965.

[18] F. A. Gibbs, W. G. Lennox, and E. L. Gibbs. The electro-encephalogram in diagnosis and in localization of epileptic seizures. *Archives of Neurology & Psychiatry*, 36(6):1225–1235, 1936.

[19] S. Herculano-Houzel. The human brain in numbers: a linearly scaled-up primate brain. *Frontiers in human neuroscience*, 3:31, 2009.

[20] B. Hjorth. Eeg analysis based on time domain properties. *Electroencephalography and clinical neurophysiology*, 29(3):306–310, 1970.

[21] T. Inouye, K. Shinosaki, H. Sakamoto, S. Toi, S. Ukai, A. Iyama, Y. Katsuda, and M. Hirano. Quantification of eeg irregularity by use of the entropy of the power spectrum. *Electroencephalography and clinical neurophysiology*, 79(3):204–210, 1991.

[22] E. R. Kandel, J. H. Schwartz, T. M. Jessell, D. of Biochemistry, M. B. T. Jessell, S. Siegelbaum, and A. Hudspeth. *Principles of neural science*. McGraw-hill New York.

[23] P. R. Kennedy, R. A. Bakay, M. M. Moore, K. Adams, and J. Goldwaithe. Direct control of a computer from the human central nervous system. *IEEE Transactions on rehabilitation engineering*, 8(2):198–202, 2000.

[24] P. R. Kleinginna and A. M. Kleinginna. A categorized list of emotion definitions, with suggestions for a consensual definition. *Motivation and emotion*, 5(4):345–379, 1981.

[25] W. Klimesch. Eeg alpha and theta oscillations reflect cognitive and memory performance: a review and analysis. *Brain research reviews*, 29(2-3):169–195, 1999.

[26] M. Kostyunina and M. Kulikov. Frequency characteristics of eeg spectra in the emotions. *Neuroscience and Behavioral Physiology*, 26(4):340–343, 1996.

[27] P. J. Lang and M. M. Bradley. International affective picture system (iaps): Technical manual and affective ratings.

[28] S. Makeig, A. J. Bell, T.-P. Jung, and T. J. Sejnowski. Independent component analysis of electroencephalographic data. In *Advances in neural information processing systems*, pages 145–151, 1996.

[29] D. J. McFarland, J. Daly, C. Boulay, and M. A. Parvaz. Therapeutic applications of bci technologies. *Brain-Computer Interfaces*, 4(1-2):37–52, 2017.

[30] S. Morgan, J. Hansen, and S. Hillyard. Selective attention to stimulus location modulates the steady-state visual evoked potential. *Proceedings of the National Academy of Sciences*, 93(10):4770–4774, 1996.

[31] J. D. Morris. Observations: Sam: the self-assessment manikin; an efficient cross-cultural measurement of emotional response. *Journal of advertising research*, 35(6):63–68, 1995.

[32] G. R. Müller-Putz, R. Scherer, G. Pfurtscheller, and R. Rupp. Eeg-based neuroprosthesis control: a step towards clinical practice. *Neuroscience letters*, 382(1-2):169–174, 2005.

[33] T. Musha, Y. Terasaki, H. A. Haque, and G. A. Ivamitsky. Feature extraction from eegs associated with emotions. *Artificial Life and Robotics*, 1(1):15–19, 1997.

[34] E. Niedermeyer and F. L. da Silva. *Electroencephalography: basic principles, clinical applications, and related fields*. Lippincott Williams & Wilkins, 2005.

[35] F. Nijboer, F. O. Morin, S. P. Carmien, R. A. Koene, E. Leon, and U. Hoffmann. Affective brain-computer interfaces: Psychophysiological markers of emotion in healthy persons and in persons with amyotrophic lateral sclerosis. In *2009 3rd international conference on affective computing and intelligent interaction and workshops*, pages 1–11. IEEE, 2009.

[36] P. L. Parmeggiani and R. A. Velluti. *The physiologic nature of sleep*. World Scientific, 2005.

[37] J. Posner, J. A. Russell, and B. S. Peterson. The circumplex model of affect: An integrative approach to affective neuroscience, cognitive development, and psychopathology. *Development and psychopathology*, 17(3):715–734, 2005.

[38] W. J. Ray and H. W. Cole. Eeg alpha activity reflects attentional demands, and beta activity reflects emotional and cognitive processes. *Science*, 228(4700):750–752, 1985.

[39] O. A. Rosso, S. Blanco, J. Yordanova, V. Kolev, A. Figliola, M. Schürmann, and E. Başar. Wavelet entropy: a new tool for analysis of short duration brain electrical signals. *Journal of neuroscience methods*, 105(1):65–75, 2001.

[40] S. J. Schiff, A. Aldroubi, M. Unser, and S. Sato. Fast wavelet transformation of eeg. *Electroencephalography and clinical neurophysiology*, 91(6):442–455, 1994.

[41] E. E. Sutter. The brain response interface: communication through visually-induced electrical brain responses. *Journal of Microcomputer Applications*, 15(1):31–45, 1992.

[42] M. Teplan et al. Fundamentals of eeg measurement. *Measurement science review*, 2(2):1–11, 2002.

[43] J. Theiler. On the evidence for low-dimensional chaos in an epileptic electroencephalogram. *Physics Letters A*, 196(1-2):335–341, 1994.

[44] Y. Tonoyan, D. Looney, D. P. Mandic, and M. M. Van Hulle. Discriminating multiple emotional states from eeg using a data-adaptive, multiscale information-theoretic approach. *International journal of neural systems*, 26(02):1650005, 2016.

[45] A. E. Vijayan, D. Sen, and A. Sudheer. Eeg-based emotion recognition using statistical measures and auto-regressive modeling. In *2015 IEEE International Conference on Computational Intelligence & Communication Technology*, pages 587–591. IEEE, 2015.

[46] M. Vourkas, S. Micheloyannis, and G. Papadourakis. Use of ann and hjorth parameters in mental-task discrimination. In *2000 First International Conference Advances in Medical Signal and Information Processing (IEE Conf. Publ. No. 476)*, pages 327–332. IET, 2000.

[47] R. L. Williams, H. W. Agnew, and W. B. Webb. Sleep patterns in young adults: An eeg study. *Electroencephalography & Clinical Neurophysiology*, 1964.

[48] B. Wittevrongel. Brain-computer interfacing based on time-domain eeg response detection combined with beamforming, 2018.

[49] J. R. Wolpaw, N. Birbaumer, D. J. McFarland, G. Pfurtscheller, and T. M. Vaughan. Brain–computer interfaces for communication and control. *Clinical neurophysiology*, 113(6):767–791, 2002.

[50] J. R. Wolpaw and D. J. McFarland. Control of a two-dimensional movement signal by a noninvasive brain-computer interface in humans. *Proceedings of the national academy of sciences*, 101(51):17849–17854, 2004.

[51] J. R. Wolpaw, D. J. McFarland, G. W. Neat, and C. A. Forneris. An eeg-based brain-computer interface for cursor control. *Electroencephalography and clinical neurophysiology*, 78(3):252–259, 1991.

[52] W.-L. Zheng, J.-Y. Zhu, Y. Peng, and B.-L. Lu. Eeg-based emotion classification using deep belief networks. In *2014 IEEE International Conference on Multimedia and Expo (ICME)*, pages 1–6. IEEE, 2014.

Master's thesis filing card

Student: Yi Zhao

Title: EEG-based photo diary app: Automatic picture taking in response to state of mind changes

UDC: 621.3

Abstract:

The past few decades have witnessed the flourishing development of brain computer interfaces (BCIs). Such systems record and analyse brain responses, and provide meaningful feedback to the user. Typical examples of BCIs are brain-controlled prosthetic limbs, mind-spelling and neuro-steered rehabilitation therapies. In recent years, affective BCIs, which aim to detect emotion from the scalp-recorded signal, have also attracted much attention since these systems not only can assist people with psychiatric disorders, but also combine with other types of BCI components to form hybrid BCI systems to achieve higher robustness. This study aims to provide theoretical proof-of-concepts for the development of an electroencephalogram (EEG)-based photo diary app. When a heightened emotional state is detected using an EEG-based emotion recognition system, a wireless webcam mounted on the EEG cap or headset would take a time-stamped picture. Such a system can assist patients with disorders of emotional information processing, and could potentially provide valuable insights for caregivers of patients with emotional disorders (e.g., autism). This study mainly analyzed the relationship between emotion and EEG signals from two perspectives: spectral power of brain rhythms (θ, α and β waves) and multivariate multiscale sample entropy (MMSE). The continuous EEG signal was divided into consecutive partly-overlapping segments, and spectral power of each segment was calculated using the Welch's algorithm. The median power value was used for representing the results of all 32 channels. It is found that the video that elicits amusement showed a significant increment of θ power and the video eliciting sadness showed a significant increment of β power. The elicitation of the emotion "anger" showed a decreased spectral power of all the three rhythms. Before applying the MMSE algorithm, 4 channels (F3, F4, P3, P4) were selected instead of all the 32 channels and a re-sample process was implemented. It is found that the MMSE feature works better in discriminating different emotions (i.e., "amusement", "anger", "sadness" and "tenderness") than in determining whether there is an emotion elicitation or not. In sum, it is anticipated that spectral power could be used in to detect a change of emotions and that the MMSE algorithm could be used for the discrimination of different emotions.

Thesis submitted for the degree of Master of Science in Artificial Intelligence, option Engineering and Computer Science

Thesis supervisor: Prof. dr. ir. Marc Van Hulle

Assessors: Dr. ir. Benjamin Wittevrongel
Dr. ir. Robin De Croon

Mentor: Dr. ir. Benjamin Wittevrongel